SECURITY BASED IMAGE PROCESSING USING SPLINES AND WAVELETS

By

Satya Prakash Ghrera

A thesis submitted for fulfillment of the requirements

for

the degree of

Doctor of Philosophy
in
COMPUTER SCIENCE & ENGINEERING

Under the Supervision of
Dr. Rajesh Siddavatam

DEPARTMENT OF COMPUTER SCIENCE & ENGINEERING
JAYPEE UNIVERSITY OF INFORMATION TECHNOLOGY,
WAKNAGHAT, SOLAN 173234 , H.P, INDIA

Roll No. 096202 **2012**

Dated: 12th March 2012

CERTIFICATE

This is to certify that **Mr. Satya Prakash Ghrera** has completed the research work for the full period prescribed by the university for Ph. D. and the thesis entitled "**Security Based Image Processing Using Splines And Wavelets"** authored by him embodies the results of his own investigations conducted during the period he worked as Ph. D. research scholar in the Department of Computer Science & Engineering, Jaypee University of Information Technology, Waknaghat, Solan, H.P, India.

Dr Rajesh Siddavatam

Associate Professor in CSE/IT

Supervisor

Acknowledgement

This thesis arose in part out of years of research that has been done at Jaypee University of IT Waknaghat, HP, India. For this research I have worked with a great number of people whose contributions in assorted ways to the research and the making of the thesis deserved special mention. It is a pleasure to convey my gratitude to them all in my humble acknowledgment.

First and foremost I offer my sincerest gratitude to my supervisor, Dr Rajesh Siddavatam, who has supported me throughout my thesis with his patience and knowledge whilst allowing me the room to work in my own way. Above all and the most needed, he provided me unflinching encouragement and support in various ways. His truly engineerist intuition has made him as a constant oasis of ideas and passions, which exceptionally inspire and enrich my growth as a student, a researcher and an engineer. I am indebted to him more than he knows. I attribute the level of my thesis to his encouragement and effort and without him this thesis, would not have been completed or written. One simply could not wish for a better or friendlier supervisor.

Many colleagues at JUIT collaborated with me for the success of this research. I would like to acknowledge the contributions of Meenakshi Arya, Rohit Verma, Ravikant Verma, P. Shyamala Jaya Sree, Pradeep Kumar and Anshul Sood. For the preparation of the thesis I have been assisted by the laboratory staff of the department of CSE and IT. I greatly acknowledge their assistance. I would also like to thank all faculty members of JUIT for their support in numerous ways.
I would like to thank the entire Administration and Management of JUIT for supporting me for this research work.

In the end, I dedicate this thesis to the memories of my father Late Sh Gita Ram Shastri, who had always been the source of inspirations for continued higher learning and achievements. I would like to express my earnest gratitude to my mother Sumana, my wife Sudeepna and my sons Aman Deep Ghrera and Raman Deep Ghrera for their support and encouragement.

(Satya Prakash Ghrera)

Table of Contents

Abstract

The main goal of the thesis is to show a novel use of the wavelet transform and singular value decomposition for enhancing the security of images through watermarking. The properties of wavelets make them special in that they have a good time and frequency localization which make them ideal for the processing of non-stationary signals like the images. The traditional Fourier transform only provides the spectral information of a signal and thus it is not suitable for the analysis of non-stationary signals. The lifting wavelet transform (LWT) is a recent approach to wavelet transform and singular value decomposition (SVD) is a valuable transform technique for robust digital watermarking. While LWT allows generating an infinite number of discrete biorthogonal wavelets starting from an initial one, singular values (SV) allow us to make changes in an image without affecting the image quality much. This thesis presents an approach which tries to amalgamate the features of these two transforms to achieve a hybrid and robust digital image watermarking techniques. Certain performance metrics are used to test the robustness of the method against common image processing attacks.

Next we show the image processing algorithms for de-noising, reconstruction and watermarking, using wavelets and splines that can be applied successfully to enhance noisy multidimensional image data sets i.e. two-dimensional (2-D) image slices and three-dimensional (3-D) image volumes. Noise removal or de-noising is an important task in image processing used to recover a signal that has been corrupted by noise. Random noise that is present in images is generated by electronic components in the instrumentation. The thesis present an Intelligent Recursive Algorithm (IRA) based on lifting filter that can efficiently remove noise. The algorithm does not

need any threshold parameters unlike the algorithms developed so far using PSM and median based filters. It is found from the results that the proposed IRA for noise removal demonstrates much better results with lesser computation time when compared to other existing algorithms. The proposed algorithm even works for binary images corrupted with impulse noise. The image restored using the proposed algorithm is compared with restoration using median based filters. It can be observed that the visual quality is much better and the finer details are very well maintained using the proposed algorithm for both binary and grayscale images

Also image representation and reconstruction methods for transmission on the network have been presented. Progressive image transmission provides a convenient User Interface when images are transmitted slowly. A progressive image reconstruction scheme based on the multi-scale edge representation of images is presented. In the multi-scale edge representation an image is decomposed into Most Significant Points which represent the strong edges and Insignificant Points which represent weak edges. Image re-construction is done based on the approximation of image regarded as a function, by a linear spline over adapted Delaunay triangulation. The proposed method progressively improves the quality of the reconstructed image till the desired quality is obtained.

Further topic of interest to be presented in the thesis is the visualization of images using some MATLAB functions. This makes it possible to visualize images without the need of special glasses especially for 3-D image volumes or using special expensive software programs which will need some bit of expertise.

The application of the proposed algorithms is mainly in the area of biomedicine, seismology, remote sensing, material science, magnetic resonance imaging (MRI) etc. as an imaging technique used primarily to produce quality images under adverse conditions of noise and security violations. The thesis presents the theory of the fundamental mathematical tools (discrete Fourier transform (DFT) and (DWT) that are used for the analysis and processing of images. The performance of the de-noising algorithms are quantitatively assessed using different criteria namely the mean square error (MSE), peak signal-to-noise ratio (PSNR) and the visual appearance. The results are discussed in accordance to the type of noise and wavelets implemented. Experimental results show that proposed de-noising and reconstruction algorithms can powerfully enhance the PSNR in noisy data sets. Finally, I conclude and give suggestions for future research work.

Keywords

Image Security, Digital image watermarking, Lifting wavelet transform, Singular value decomposition, Progressive image transmission, Delaunay triangulation, Linear Bivariate splines, Image restoration, Impulse Noise, Binary Images, Salt and Pepper Noise, Median Filter, Time-Frequency and Time-Scale Signal Analysis, Discrete Wavelet Transform, Complex Wavelet Transform, Biorthogonal wavelets, Segmentation, Feature Extraction, Visualization

List of Figures

List of Tables

Chapter 1
Introduction

Image processing can be defined as the manipulation of an image for the purpose of either extracting information from the image or producing an alternative representation of the image. There are numerous specific motivations for image processing but many fall into the following categories:

(i) To secure the image against attacks on image integrity or copyright violations.

(ii) To remove unwanted signal components that are corrupting the image.

(iii) To extract information by rendering it in a more obvious or more useful form.

An image can be defined as a two dimension function f (x, y) (2D Image), where x and y are spatial coordinates, and the amplitude of f at any pair of (x, y) is gray level of the image at that point. For example, a grey level image can be represented as:

$$f\,ij \text{ Where } f\,ij \equiv f\,(x_i, y_j)$$

When x, y and the amplitude value of f are finite, discrete quantities, the image is called "a digital image"[61]. The finite set of digital values is called *picture* *elements* or pixels. Typically, the pixels are stored in computer memory as a two dimensional array or matrix of real number.

In the thesis we present a robust watermarking technique for image security. Watermark may be embedded either in spatial domain or in transform domain. Transform domain techniques employ various transforms. In order to have more promising techniques, researches were directed towards watermarking in the transform domain, where the watermark is not added to the image intensities, but to the values of its transform coefficients. Then to get the watermarked image, one should perform the transform inversely. Wavelet based transforms gained popularity recently because of the property of multiresolution analysis that it provides. A new approach to wavelet transform is the lifting wavelet transform[19]. In this thesis, the fusion of LWT and SVD approaches i.e. LWT-SVD scheme is proposed, where an image is watermarked using other image for the purpose of validation. The purpose of singular value decomposition is to reduce a dataset containing a large number of values to a dataset containing significantly fewer values, but which still contains a large fraction of the variability present in the original data. SVD analysis results in a more compact representation of these correlations, especially with multivariate datasets and can provide insight into spatial and temporal variations exhibited in the fields of data being analyzed.

Next we present an efficient scheme for noise removal. Noise should be removed while keeping the fine details of the image intact. An intelligent recursive noise removal algorithm (IRA) based on the lifting filter that can efficiently remove noise is presented in this thesis. The algorithm computes the threshold and demonstrates superior results with lesser computation time. Noise in images consists of random signals that do not come from the source object but from other sources in the machine and environment that do not contribute to the image differentiation. The noise of an image gives it a grainy appearance and mainly the noise is evenly spread and more uniform. It is often desirable to process it to enhance the visibility of certain features such as the edges. There are many advanced methods of image processing involving techniques that include the traditional Fourier transform and the wavelet transform. Recently a dual tree complex wavelet transform (DT CWT) was developed and has added advantages over classical methods, these include shift invariance and improved directionality. In this thesis we propose the lifting scheme with improved PSNR. Experiments are done on 2-D image data sets. The performance of the de-noising algorithms are quantitatively assessed using different criteria namely the PSNR, MSE and the visual appearance.

In this thesis we also propose a new scheme for image data representation. Although image compression provides an efficient and effective method to reduce the amount of data needed to represent an image, it oftentimes requires receivers to wait for the completely encoded results before reconstructing the image. If the decoded image is not the expected one, then receivers must transmit another image again. Progressive Image Transmission (PIT) techniques have been proposed to alleviate this problem by first sending a coarse version of the original image and then resending it progressively. Progressive image transmission can help reducing the latency when transmitting raster images over low bandwidth links. Often, a rough approximation (preview) of an image is sufficient for the user to decide whether or not it should be transmitted in greater detail. This allows the user to decide whether to wait for a more detailed reconstruction, or to abort the transmission. Progressive image transmission has many applications, such as teleconferencing, remote image database access and so on. Accordingly, A Fast Progressive Image Transmission Algorithm Using Linear Bivariate Splines has been proposed.

1.1 Objectives

The main objectives of the thesis can be summarized as follows:

- The lifting wavelet transform (LWT) and singular value decomposition (SVD) techniques for robust digital watermarking.
- Intelligent Recursive Algorithm (IRA) based on lifting filter that can efficiently remove noise.
- Progressive image reconstruction scheme based on the multi-scale edge representation using linear bivariate splines.

1.2 Key Concepts

Key concepts relevant for research are given below. These concepts have been discussed in subsequent paragraphs.

(a) Singular Value Decomposition.

(b) Wavelet Transforms

(c) Lifting Scheme

(d) Linear Bivariate Splines

1.3 Singular Value Decomposition.

The singular value decomposition of nxp matrix A is its representation as $A = U W V^T$, where U is an orthogonal nxn matrix, V - orthogonal pxp matrix[14]. The diagonal elements of matrix *W* are non-negative numbers in descending order, all off-diagonal elements are zeros.

$$\begin{pmatrix} \cdot & \cdot & \cdot \\ \cdot & \cdot & \cdot \\ \cdot & A & \cdot \\ \cdot & \cdot & \cdot \\ \cdot & \cdot & \cdot \end{pmatrix} = \begin{pmatrix} \cdot & \cdot & \cdot & \cdot & \cdot \\ \cdot & \cdot & \cdot & \cdot & \cdot \\ \cdot & \cdot & U & \cdot & \cdot \\ \cdot & \cdot & \cdot & \cdot & \cdot \\ \cdot & \cdot & \cdot & \cdot & \cdot \end{pmatrix} \begin{pmatrix} w_1 & & \\ & w_2 & \\ & & w_3 \\ & & \\ & & \end{pmatrix} \begin{pmatrix} \cdot & \cdot & \cdot \\ \cdot & V^T & \cdot \\ \cdot & \cdot & \cdot \end{pmatrix}$$

The matrix *W* consists mainly of zeros, so we only need the first min(n,p) columns of matrix *U* to obtain matrix *A*. Similarly, only the first min(n,p) rows of matrix V^T affect the product. These columns and rows are called left and right singular vectors. SVD allows us refactoring a digital image in three matrices. The using of singular values of such refactoring allows us to represent the image with a smaller set of values, which can preserve useful features of the original image, but use less storage space in the memory, and achieve the image compression process.

Singular value decomposition takes a rectangular matrix of image data (defined as A, where A is a *n* x *p* matrix) in which the *n* rows and the *p* columns represents the experimental conditions. The SVD theorem states:

$$\mathbf{A}_{nxp} = \mathbf{U}_{nxn}\, \mathbf{W}_{nxp}\, \mathbf{V}^{T}_{pxp}$$

Where

$\mathbf{U}^T\mathbf{U} = \mathbf{I}_{nxn}$

$\mathbf{V}^T\mathbf{V} = \mathbf{I}_{pxp}$ (i.e. U and V are orthogonal)

Where the columns of U are the left singular vectors; W (the same dimensions as *A*) has singular values and is diagonal; and V^T has rows that are the right singular vectors. The SVD represents an expansion of the original data in a coordinate system where the covariance matrix is diagonal.

Calculating the SVD consists of finding the eigenvalues and eigenvectors of AA^T and A^TA. The eigenvectors of A^TA make up the columns of V , the eigenvectors of AA^T make up the columns of U. Also, the singular values in **W** are square roots of eigenvalues from AA^T or A^TA. The singular values are the diagonal entries of the W matrix and are arranged in descending order. The singular values are always real numbers. If the matrix A is a real matrix, then U and V are also real.

Proof:

$\mathbf{A}=\mathbf{UWV}^{\mathrm{T}}$ and $\mathbf{A}^{\mathrm{T}}=\mathbf{VWU}^{\mathrm{T}}$

$\mathbf{A}^{\mathrm{T}}\mathbf{A} = \mathbf{VWU}^{\mathrm{T}}\mathbf{UWV}^{\mathrm{T}}$

$\mathbf{A}^{\mathrm{T}}\mathbf{A} = \mathbf{VW}^2\mathbf{V}^{\mathrm{T}}$

$\mathbf{A}^{\mathrm{T}}\mathbf{AV} = \mathbf{VW}^2$

There are many properties and attributes of SVD, such as:

1. The singular value of W are unique, however, the matrices *U and V* are not unique;
2. Since $A^T A = VW^T WV^T$, so V diagonalizes $A^T A$, it follows that the $\mathbf{v}j$'s are the eigenvector of $A^T A$.
3. Since $AA^T = UWW^T U^T$, so it follows that U diagonalizes AA^T and that the u_i *'s* are the eigenvectors of AA^T .
4. If A has rank of r then $\mathbf{v}j$, $\mathbf{v}j$, …, $\mathbf{v}r$ form an orthonormal basis for range space of A^T ,$R(A^T$), and $\mathbf{u}j$, $\mathbf{u}j$, …, $\mathbf{u}r$ form an orthonormal basis for range space *A*, $R(A)$.
5. The rank of matrix A is equal to the number of its nonzero singular values.

The property 5 of the SVD may be applied for image compression which deals with the problem of reducing the amount of data required to represent a digital image. Compression is achieved by the removal of three basic data redundancies:

1. Coding redundancy, which is present when less than optimal.
2. Interpixel redundancy, which results from correlations between the pixels.
3. Psycho visual redundancies, which is due to data that is ignored by the human visual.

The property 5 of SVD tells us "the rank of matrix A is equal to the number of its nonzero singular values". In many applications, the singular values of a matrix decrease quickly with increasing rank. This propriety allows us to reduce the noise or compress the matrix data by eliminating the small singular values or the higher ranks. When an image is SVD transformed, it is not compressed, but the data take a form in which the first singular value has a great amount of the image information. With this, we can use only a few singular values to represent the image with little differences from the original.

To illustrate the SVD image compression process, we show detail procedures:

$A=UWV^T=\sum_{i=1}^{r} \sigma_i u_i v_i^T$

That is *A* can be represented by the outer product expansion:

$A= \sigma_1 u_1 v_1^T + \sigma_2 u_2 v_2^T + \dots\dots.. \sigma_r u_r v_r^T$

When compressing the image, the sum is not performed to the very last SVs, the SVs with small enough values are dropped (the SVs are ordered on the diagonal).

The closet matrix of rank *k* is obtained by truncating those sums after the first *k* terms:

$A_k = \sigma_1 u_1 v_1^T + \sigma_2 u_2 v_2^T + \ldots\ldots.. \sigma_k u_k v_k^T$

The total storage for A_k will be $k\ (m + n + 1)$. The integer *k* can be chosen confidently less then *n,* and the digital image corresponding to A_k will still have very close the original image. However, each different *k* will have a different corresponding image and storage for it.

Image Compression Measurement

To measure the performance of the SVD image compression method, we can compute the compression factor and the quality of the compressed image. Image compression factor can be computed using the Compression ratio:

$$C_k = \frac{m.n}{k(m+n+1)}$$

To measure the quality between original image *A* and the compressed image A_k , the measurement of Mean Square Error (MSE) can be computed:

$$MSE=\frac{1}{m.n}\sum_{y=1}^{m}\sum_{x=1}^{n}[\ [f_A(x,y)-f_{Ak}(x,y)]$$

On a computer, an image is simply a matrix denoting pixel colors. For example, a grayscale image can be represented as a matrix whose entries are integers between 0 and 255 (for 256 shades of gray), denoting the shade of each pixel. Typically, such matrices can be well-approximated by low-rank matrices. Instead of storing the mn entries of the matrix A, one need only store the k(m + n) + k numbers that make up the various σ_j , u_j , and v_j values in the sum

$A=USV^T=\sum_{i=1}^{k} \sigma_i u_i v_i^T$

When k<<min(m, n), this can make a significant improvement.

1.4 Wavelet Transforms

As a mathematical tool, wavelets can be used to extract information from many different kinds of data, including audio signals and images[75]. Sets of wavelets are generally needed to analyze data fully. A set of "complementary" wavelets will deconstruct data without gaps or overlap so that the deconstruction process is mathematically reversible. Thus, sets of complementary wavelets are useful in wavelet based compression/decompression algorithms where it is desirable to recover the original information with minimal loss.

1.4.1 Time-Frequency Analysis

Time-frequency analysis plays a central role in signal analysis. The Fourier Transform (FT) is only suitable for stationary signals, i.e., signals whose frequency content does not change with time. Fourier analysis is not well suited to describing local changes in frequency content because the frequency components defined by the Fourier transform have infinite (i.e. global) time support. The time representation is usually the first description of a signal $s(t)$ obtained by a receiver recording variations with time. The frequency representation, which is obtained by the well known Fourier transform (FT)[58], highlights the existence of periodicity, and is also a useful way to describe a signal.

The relationship between frequency and time representations of a signal can be defined as:

$$S(\nu)=\int_{-\infty}^{+\infty}s(t)e^{-j2\pi\nu t}dt, \qquad s(t)=\int_{-\infty}^{+\infty}S(\nu)e^{j2\pi t\nu}d\nu$$

Figure 1.1 shows the graphical representation a typical time frequency analysis.

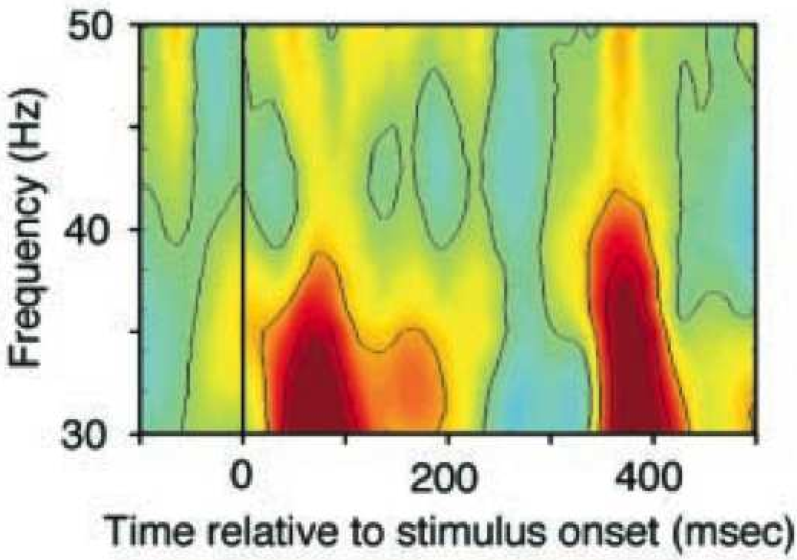

Figure 1.1: Time Frequency Analysis[57]

1.4.2 Discrete Fourier Transform

Discrete Fourier transform (DFT) plays a central role in the implementation of many signal and image processing algorithms. DFT is a mathematical transform which resolves a time series $x(n)$ into the sum of an average component and a series of sinusoids with different amplitudes and frequencies. The N-point DFT, $X(k)$, of an N-point discrete time sequence, $x(n)$, is defined as:

$$X(k)=\sum_{N=0}^{N-1} X(n).e^{-j2\Pi kn/N} \qquad (1)$$

for $k = 0, 1, \ldots, N - 1$. The inverse of the DFT is defined as:

$$X(n)=\frac{1}{N}\sum_{k=0}^{N-1} X(k).e^{-j2\Pi kn/N} \qquad n = 0, 1, \ldots, N-1 \qquad (2)$$

From Eq. (1) it can be seen that the computation of $X(k)$ requires N^2 complex multiplications, thus the DFT is an $O(N^2)$ process. An algorithm was developed byTukey and Cooley in 1965 called Fast Fourier Transform (FFT) that speeds up the process by computing the DFT using $O(N \log N)$ operations.

Two-dimensional discrete Fourier transform is used for the processing of images. Basis functions are sinusoids with frequency u in one direction times sinusoids with frequency v in the other. For an $M \times N$ image $\boldsymbol{f}[m, n]$, these basis functions can be replaced for computational purposes by complex exponentials $e^{i2\pi um/M}$ and $e^{i2\pi vn/N}$ to evaluate the discrete Fourier transform. The 2-D DFT for an $M \times N$ is usually defined as:

$$F(u,v)=\sum_{m=0}^{M-1}\sum_{n=0}^{N-1} f(m,n).e^{i2\Pi\,(um/M+un/N)} \qquad (3)$$

and its inverse transform is:

$$F(u,v)=\frac{1}{M.N}\sum_{u=0}^{M-1}\sum_{v=0}^{N-1} f(u,v).e^{i2\Pi(um+vn)} \qquad (4)$$

where $F[u, v]$ is the spectrum of the image in the frequency domain and $m = 0$, 1, $\ldots$, $M-1$, $n = 0, 1, \ldots, N-1$, $u = 0, 1, \ldots, M-1$, $v = 0, 1, \ldots, N-1$ are all discrete variables.

Filtering may be achieved in the transform domain by first computing the DFT, applying a filter which modifies the transform values, and then applying an inverse transform. The image $f(x, y)$ is first transformed to give $F(u, v)$ and finally the transform is modified using the equation below;

$$G(u, v) = H(u, v)\ F(u, v)$$

where $H(u, v)$ is the filter function. The filtered transformed is then inverse-transformed to give the filtered image $g(x, y)$.

1.4.3 Time-Scale Analysis

The Continuous Wavelet Transform (CWT) provides a time-scale description similar to that of the short time Fourier transform (STFT) with a few important differences: frequency is related to scale and the CWT is able to resolve both time and scale (frequency) events better than the STFT. Wavelet series are thus constructed with two parameters scale and translation, these parameters make it possible to analyze a signal behavior at a dense set of time locations and with respect to a vast range of scales, thus providing the ability to zoom in on the transient behavior of the signal. The CWT[69] is defined as the convolution of $x(t)$ with a wavelet function, $W(t)$, shifted in time by a translation parameter b and a dilation parameter a (Eq. 5).

$$X_w(a,b)=\frac{1}{\sqrt{a}}\int_{-\infty}^{+\infty} w\left(\frac{t-b}{a}\right)x(t)dt \qquad (5)$$

Figure 1.2 shows the Wavelet functions in time and frequency domain.

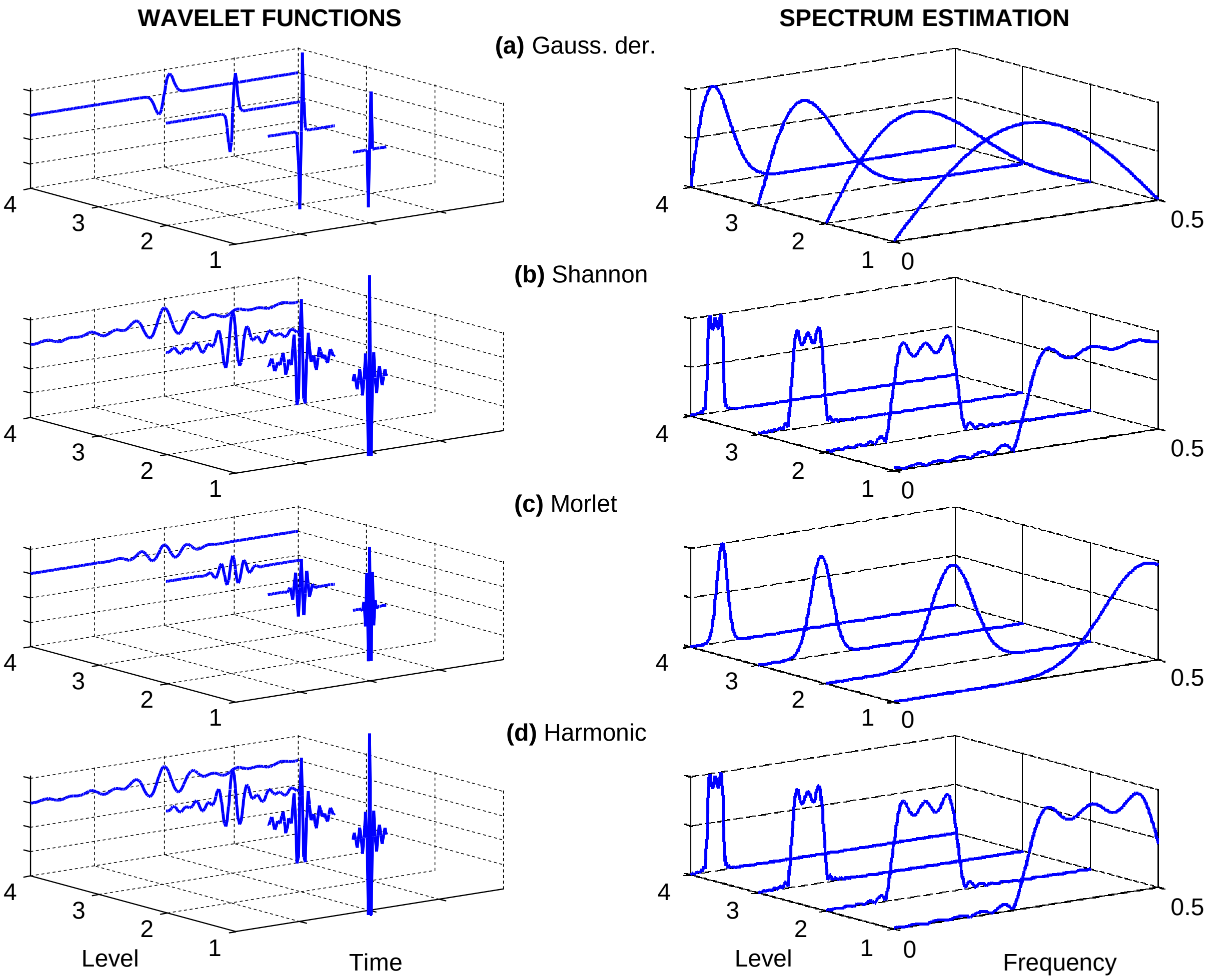

Figure 1.2: Wavelet functions in time and frequency domain[72]

1.4.4 Discrete Wavelet Transform

CWT is redundant since the parameters (a, b) are continuous thus it's necessary to discretize the grid on the time-scale plane corresponding to a discrete set of continuous basis functions. This leads us to a question: how can we discretize the wavelet in Eq. (5)?

$$W_{j,k}(t)=\frac{1}{\sqrt{aj}}W\left(\frac{t-bk}{aj}\right) \qquad (6)$$

In theory $a_j = a^j{}_0$ and $b_k = kb_0a^j$ where $j, k \in Z$, $a_0 > 1$, $b_0 = 0$.

The discrete form of the wavelet is shown in Eq. (6), where j controls the dilation and k controls the translation.

Wavelet analysis is simply the process of decomposing a signal into shifted and scaled versions of a mother (initial) wavelet. An important property of wavelet analysis is perfect reconstruction, which is the process of reassembling a decomposed signal or image into its original form without loss of information.

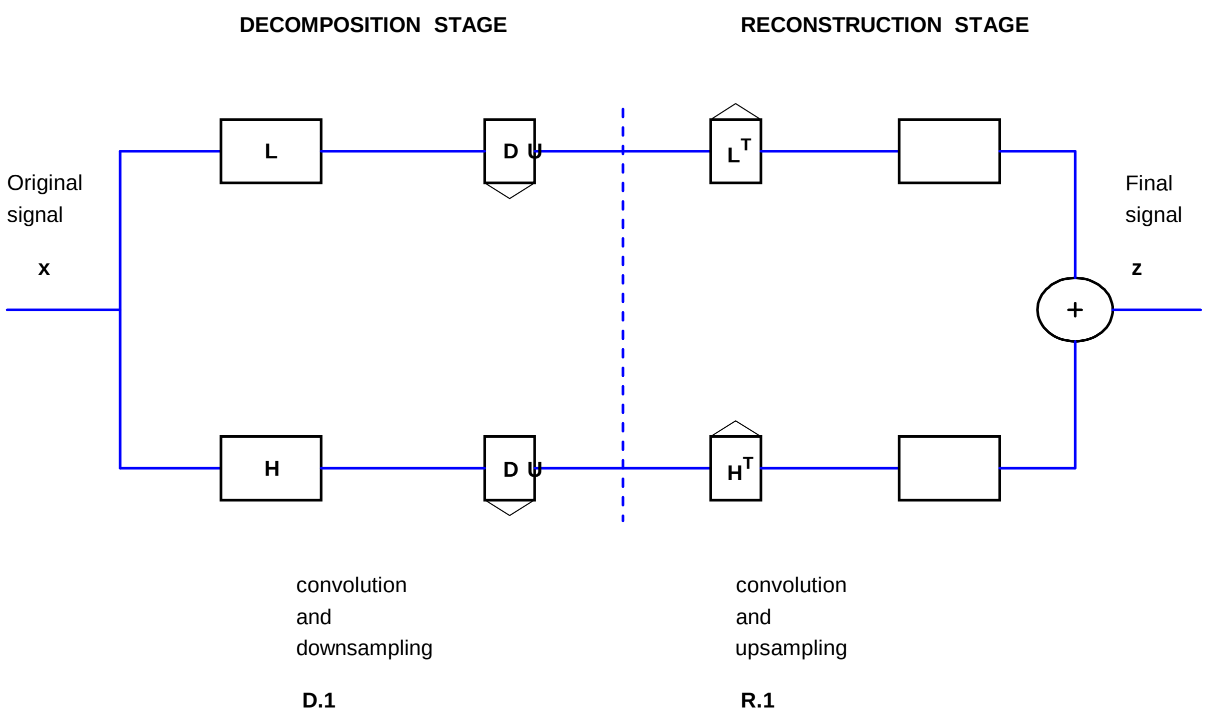

Figure 1.3: Signal decomposition and reconstruction[76]

In Figure 1.3, L and H represent the scaling function and wavelet function respectively. A pair of filters: a low-pass filter L and a high-pass filter H, split a signal's bandwidth in two halves. This provides the coefficients $c_j(k)$ and $d_j(k)$ for the decomposition of the signal into its scaling function and wavelet function components. The inverse discrete wavelet transform (IDWT) reconstructs a signal from the approximation and detail coefficients derived from decomposition. The right side of Figure 1.3 shows an example of reconstruction.

1.4.5 Two dimensional Discrete Wavelet Transform

Digital images are 2-D signals that require a two-dimensional wavelet transform. The 2-D DWT[68] analyzes an image across rows and columns in such a way as to separate horizontal, vertical and diagonal details. In the first stage [76] the rows of an $N \times N$ are filtered using a high pass and low pass filters. In the second stage 1-D convolution of the filters with the columns of the filtered image is applied. Each of the branches in the tree is shown in the Figure 1.6 therefore produces an $(N/2) \times (N/2)$ subimage. This leads at each level to 4 different subbands HH, HL, LH and LL . The LL is filtered again to get the next level representation, Figure 1.6 summarizes the transform for a one level decomposition.

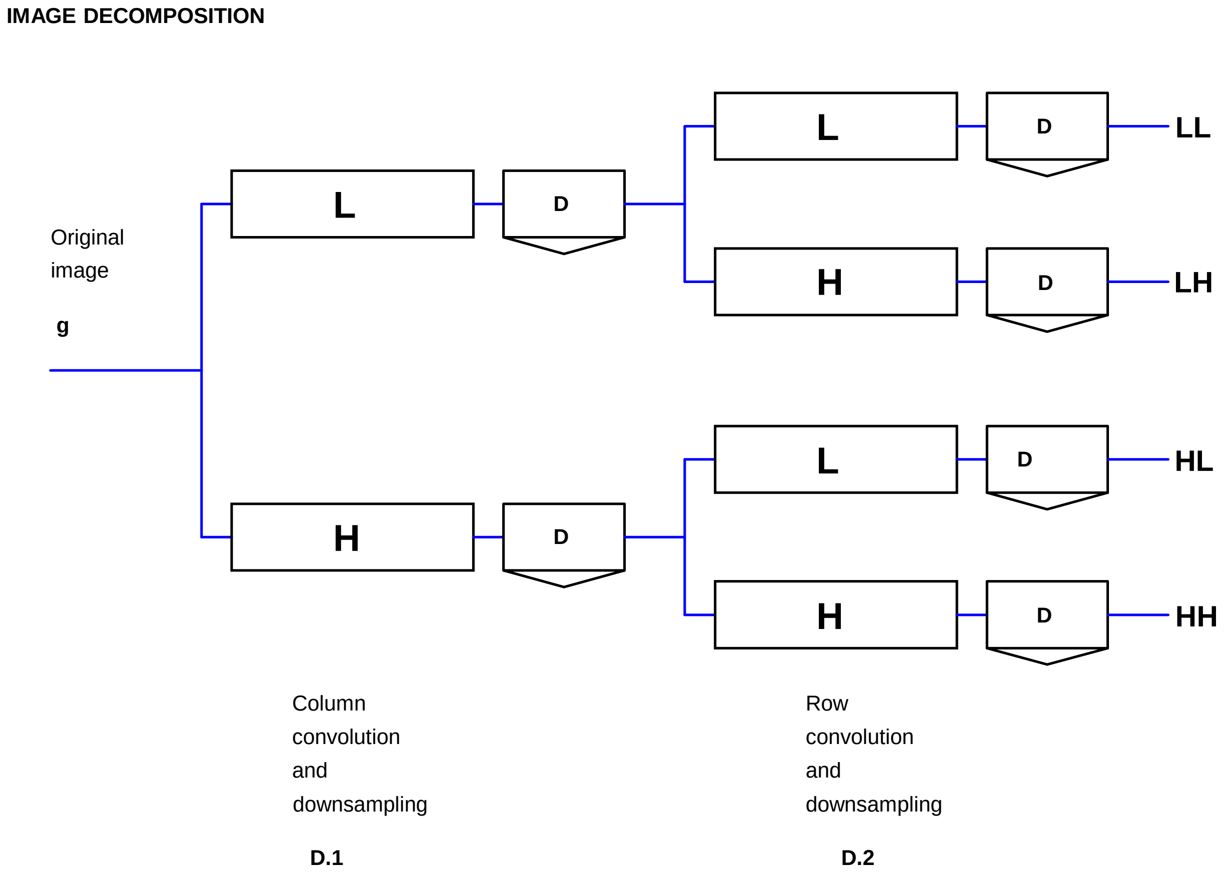

Figure 1.4: A one-level two-dimensional DWT decomposition[57]

To reconstruct the image from its 2-D DWT subimages (LH, HL,HH) the details are recombined with the low pass approximation using upsampling and convolution with the respective synthesis filters. Upsampling refers to the insertion of a zero row after each existing row or a zero column after each existing column.

1.4.6 Three-dimensional Discrete Wavelet Transform

DWT is a separable, sub-band transform. 3-D wavelets [67],[73-74] can be constructed as separable products of 1-D wavelets by successively applying a 1-D analyzing wavelet in three spatial directions (x, y, z). The volume $F(x, y, z)$ is first filtered along the x-dimension, resulting in a low-pass image $L(x, y, z)$ and a high-pass image $H(x, y, z)$. Both L and H are then filtered along the y-dimension, resulting in four decomposed sub- volumes: LL, LH , HL and HH. Then each of these four subvolumes are filtered along the z-dimension, resulting in eight sub-volumes: LLL, LLH, LHL, LHH, HLL, HLH, HHL and HHH.

1.4.7 Dual Tree Complex Wavelet Transform

The dual-tree complex wavelet transform (CWT) is a relatively recent enhancement to the discrete wavelet transform (DWT), with important additional properties: It is nearly shift invariant and directionally selective in two and higher dimensions. It achieves this with a redundancy factor of only 2*d* for *d*-dimensional signals, which is substantially lower than the undecimated DWT. The multidimensional (M-D) dual-tree CWT is nonseparable but is based on a computationally efficient, separable filter bank (FB). This tutorial discusses the theory behind the dual-tree transform, shows how complex wavelets with good properties can be designed, and illustrates a range of applications in signal and image processing.

Different wavelet techniques can be successfully applied in various signal and image processing methods, namely in image de-noising, segmentation, classification and motion estimation. The 1-D dual-tree wavelet transform is using a pair of filter banks operating on the same data simultaneously. The upper iterated filter bank represents the real part of a complex wavelet transform. The lower one represents the imaginary part as shown in Figure 1.5 below.

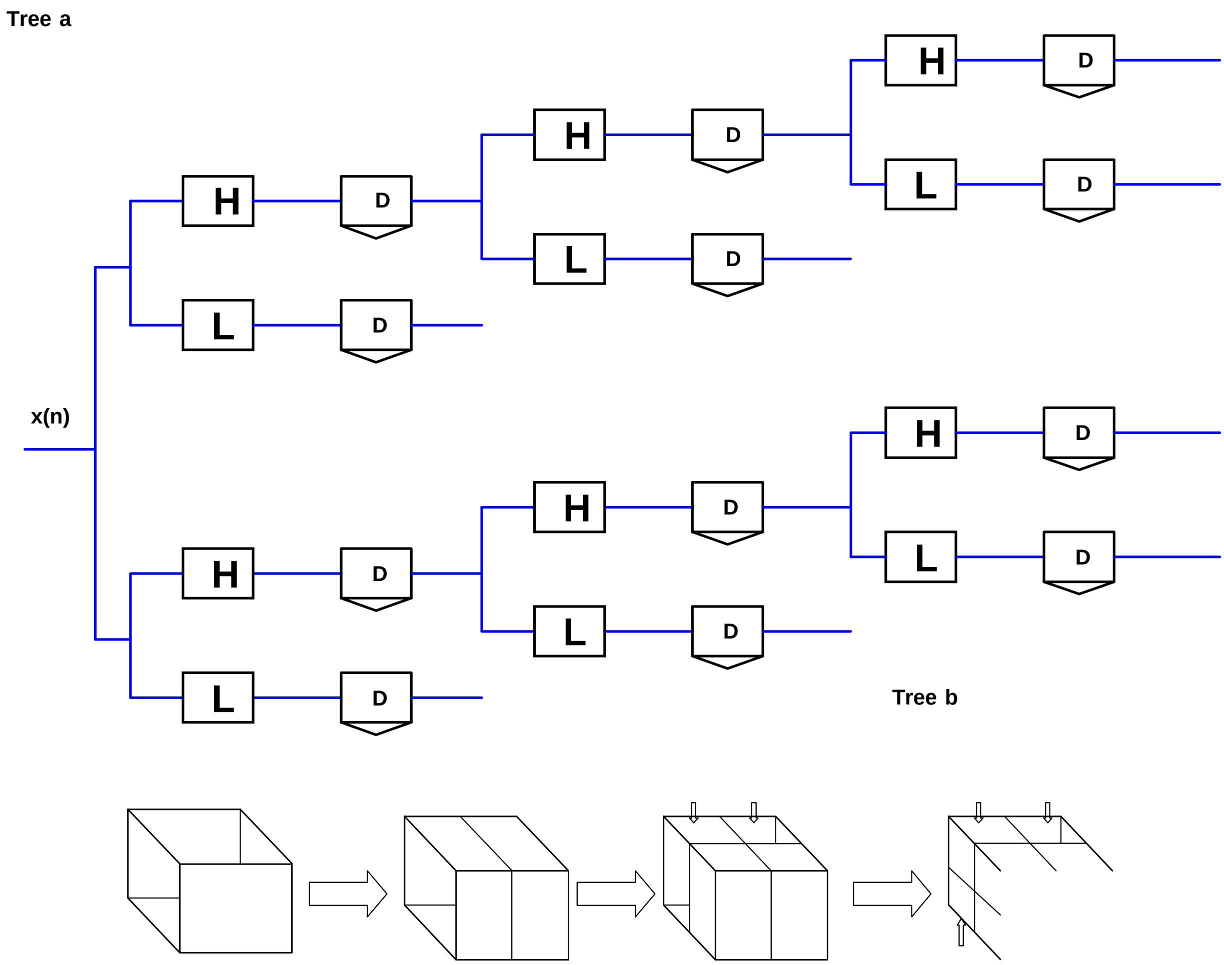

Figure 1.5: The 1-D dual-tree complex wavelet transform[61].

1.5 Lifting Scheme

The lifting scheme is a technique for both designing wavelets and performing the discrete wavelet transform. Actually it is worthwhile to merge these steps and design the wavelet filters *while* performing the wavelet transform. This is then called the second generation wavelet transform. The technique was introduced by Wim Sweldens. The wavelet Lifting Scheme is a method for decomposing wavelet transforms into a set of stages. Lifting scheme algorithms have the advantage that they do not require temporary arrays in the calculations steps and have less computations using the lifting coefficients to represent the discrete wavelet transform kernel. Lifting scheme as shown in Figure 1.6 involves steps as under.

1. Splitting Step

$s_i^0 \longrightarrow x_{2i}$, $d_i^0 \longrightarrow x_{2i+1}$

2. Lifting Step

$d_i^0 = d_i^0 - \frac{1}{2}(s_i^0 + s_{i+1}^0)$ (predict step)

$s_i^1 = s_i^0 - \frac{1}{4}(d_{i-1}^1 + d_i^1)$ (update step)

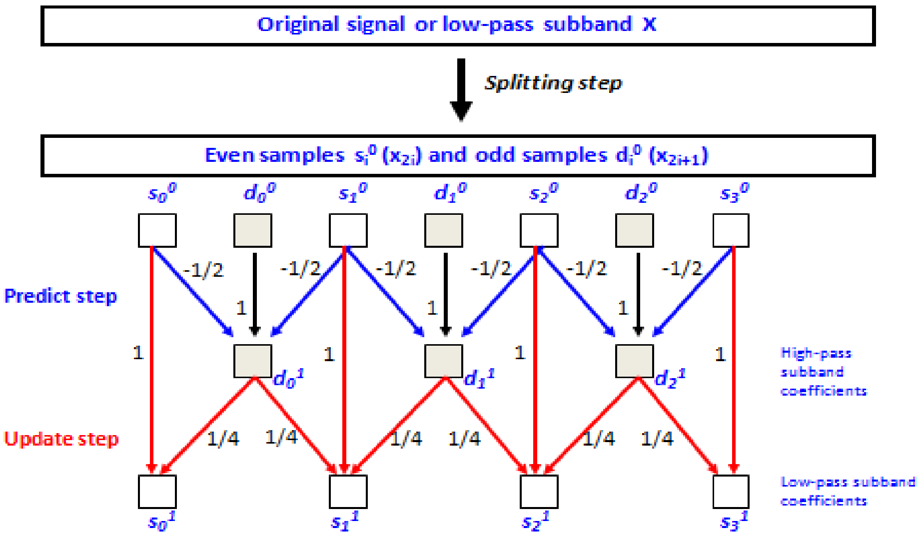

Figure 1.6: Lifting Scheme[19].

1.6 Linear Bivariate Splines

Bivariate splines[30] can be used as a fundamental tool for approximating any known or unknown functions. Typical applications are scattered data fitting. and interpolations, numerical solutions of partial differential equations, image enhancements, and data forecasting. The fundamental idea behind spline interpolation is based on the engineer's tool used to draw smooth curves through a number of points. This spline consists of weights attached to a flat surface at the points to be connected. A flexible strip is then bent across each of these weights, resulting in a pleasingly smooth curve. The mathematical spline is similar in principle. The points, in this case, are numerical data. The weights are the coefficients on the polynomials used to interpolate the data. These coefficients 'bend' the line so that it passes through each of the data points without any erratic behavior or breaks in continuity.

An interval [a..b] is subdivided into sufficiently small intervals $[\xi_j..\ \xi_{j+1}]$, with

$a=\xi_1<\ldots<\xi_{l+1}=b$. On each such interval, a polynomial p_j of relatively low degree can provide a good approximation to g. This can even be done in such a way that the polynomial pieces blend smoothly, i.e. so that the resulting composite function s(x) that equals $p_j(x)$ for $x\in[\xi_j\ \xi_{j+1}]$, for all j , has several continuous derivatives. Any such smooth piecewise polynomial function is called a *spline*. If f is a function of x, and g is a function of y, then their tensor-product p(x,y):=f(x)g(y) is a function of x and y. For a bivariate spline of order h in x and k in y, we have:

Knot sequences

- $s=(s_1,\ldots,s_{m+h})$
- $t=(t_1,\ldots,t_{n+k})$

Coefficients (a_{ij}:i=1..m, j=1..n)

Linear bivarite function may be represented as

$$f(x,y)=\sum_{i=1}^{m}\sum_{j=1}^{n}B(x\,|\,s_i,\ldots,s_{i+h})B(y\,|\,t_j,..,t_{j+k})a_{ij}$$

Chapter 2

A Hybrid Semi-Blind Digital Image Watermarking Technique

2.1 Introduction

There has been an upsurge in broadcasting media since the beginning of this century because of many technical innovations in this field. Media security concerns are copyright protection, broadcast monitoring and owner identification. Digital watermarking is the greatest bet to address these concerns . The ease of distribution of documents through the web may transgress protection laws against unauthorized copies and make fidelity questionable. Digital watermarking has been proposed as a solution against these practices. Digital watermarking is a labeling technique of digital data with secret information that can be extracted in the receptor. The image in which this data is inserted is called cover image or host. The watermarking process has to be resilient against all possible attacks, keeping the content of the watermark readable in order to be recognized when extracted. Features like robustness and fidelity are essentials for a watermarking system, however the size of the embedded information has to be considered since data becomes less robust as its size increases. Therefore a trade-off of these features must be considered. In this thesis, we show a classification of watermarks, propose a basic model for watermarking and explain efficient algorithms for image watermark embedding and extraction.

2.2 Detection Types

This classification determines which resources are necessary for the analysis to extract the watermark from the cover image.

1) Blind: In this detection type the original image and mark data is not available to the receiver. For example: Copy control applications must send different watermarks for each user and the receiver must be able to recognize and interpret these different marks.

2) Non-Blind: In this case, the receiver needs the original data, or some derived information from it, for the detection process [1]. This data will also be used in the extraction algorithm.

The lifting wavelet transform (LWT) is a recent approach to wavelet transform and singular value decomposition (SVD) is a valuable transform technique for robust digital watermarking. While LWT allows generating an infinite number of discrete biorthogonal wavelets starting from an initial one, singular values (SV) allow us to make changes in an image without affecting the image quality much. This paper presents an approach which tries to amalgamate the features of these two transforms to achieve a hybrid and robust digital image watermarking techniques. Certain performance metrics are used to test the robustness of the method against common image processing attacks. Copyright Protection is a major issue as far as content transfer over the worldwide web is concerned. There is a growing concern over multimedia content protection with the growing accessibility and usability of internet. Major issue of concern here is the images, audio or video transmitted. Various methods address this issue of multimedia content protection, one of them being digital image watermarking[77-100]. Watermarking (data hiding) [1, 2, 3] is the process of embedding data into a multimedia element such as image, audio or video. This embedded data can later be extracted from, or detected in, the multimedia for security purposes[101-110].

Digital watermarking is the process of possibly irreversibly embedding information into a digital signal. The signal may be audio, pictures or video, for example. If the signal is copied, then the information is also carried in the copy. In visible watermarking, the information is visible in the picture or video. Typically, the information is text or a logo which identifies the owner of the media. In invisible watermarking, information is added as digital data to audio, picture or video, but it cannot be perceived as such. The digital watermarking is intended to complement cryptographic process. Access control or authenticity verification has been addressed by digital watermarking as well as by biometric authentication [4].

2.3 Watermark Embedding

The method used to embed the watermark influence both the robustness against attacks and the detection algorithm, but some methods are very simple and cannot meet the application requirements. El-Gayyar and von zur Gathen[111] showed that designing a watermark should consider a trade-off among the basic features of robustness, fidelity and payload. There are two approaches for the embedding process:

1) **Spatial Domain:** These watermarks insert data in the cover image changing pixels or image characteristics. Watermark is embedded using LSB, Statistical, Feature based and Block based techniques. Spatial-domain techniques work with the pixel values directly. The algorithms should carefully weight the number of changed bits in the pixels against the possibility of the watermark becoming visible. These watermarks have been used for document authentication and tamper detection. Generally, spatial domain watermarking is easy to implement from a computational point of view, but too fragile to resist numerous attacks [5].

2) **Transform Domain:** These algorithms hide the watermarking data in transform coefficients, therefore spreading the data through the frequency spectrum making it hard to detect and strong against many types of signal processing manipulations. The most used transforms are: Discrete cosine transform (DCT) , Discrete Fourier Transform (DFT), discrete wavelet transform (DWT) and discrete lifting transform (LWT) like the ones suggested in [6,7].

2.4 Transform Domain Watermarking Algorithms

Transform-domain techniques employ various transforms, either local or global. In order to have more promising techniques, researches were directed towards watermarking in the transform domain, where the watermark is not added to the image intensities, but to the values of its transform coefficients. Then to get the watermarked image, one should perform the transform inversely.

In case of frequency domain watermarking schemes, there has to be a trade-off between robustness and invisibility. When a watermark is embedded in the most significant components, it becomes robust to attacks but the watermark becomes difficult to hide. Whereas, when we embed a watermark in the lesser significant components, it is easier to hide it but the scheme is least resistant to attacks.

The wavelet transform is one type of transform domain technique. Wavelet based transforms gained popularity recently because of the property of multi-resolution analysis that it provides. Wavelets can be orthogonal or bi-orthogonal. Most of the wavelets used in watermarking are orthogonal wavelets. A new approach to wavelet transform is the lifting wavelet transform [20]. In this paper, the fusion of LWT and SVD approaches i.e. LWT-SVD scheme is proposed, where an image is watermarked using other image for the purpose of validation.

2.5 Watermarking technique using LWT and SVD

The decomposition of a signal in terms of a wavelet basis is termed as wavelet transform. The basic idea of wavelet transforms is to exploit the correlation structure present in most real life signals to build a sparse approximation. A new mathematical formulation proposed by Swelden [20], based on spatial construction of the wavelets is called the lifting-based wavelet transform. The underlying principle of this approach [19,20] is to break up the high- pass and the low -pass wavelet filter into a sequence of smaller filters that in turn can be converted into a sequence of alternating upper and lower triangular matrices and a diagonal matrix with constants. The factorization is obtained by using an extension of the Euclidean algorithm. The resulting formulation can be implemented by means of banded matrix multiplications.

Let $h(z)$ and $g(z)$ be the low pass and high pass analysis filters and $h(z)$ and $g(z)$ be the low pass and high pass synthesis filters. The polyphase representation of the filter h is expressed as depicted in equation 1 and Figure 2.1 .

$$h(z) = h(z^2) + z^{-1} h(z^2) \qquad (1)$$

First subsample into even and odd, then apply the dual polyphase matrix. For the inverse transform, First apply the polyphase matrix and then join even and odd.

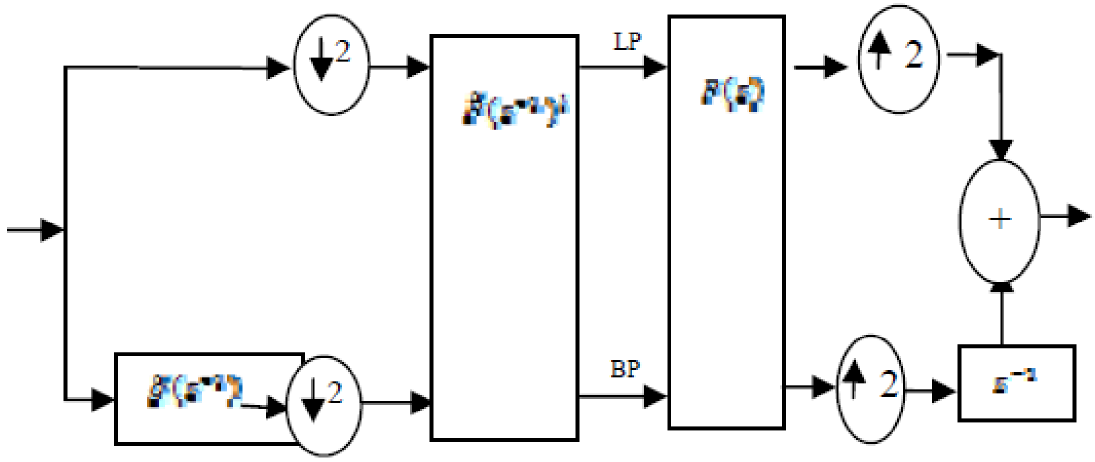

Figure 2.1: Polyphase representation of wavelet transform

The lifting scheme [20] is an easy relationship between perfect reconstruction filter pairs that have the same low-pass or high-pass filter. One can then start from the Lazy wavelet and use lifting to gradually build one's way up to a multiresolution analysis with particular properties. The lifting technique used in the present approach is Primal Lifting, which lifts the low-pass sub-band with the help of high- pass sub-band.

The Singular Value Transform (SVD), was explored a few years ago for watermarking purposes. In recent years, SVD has been used in watermarking as a different transform as it is one of the most powerful tools of linear algebra with several applications in image compression [8,9,10,11,12,13], watermarking[14,15,16,17]. Singular values are the luminance values of SVD image layer, changing these values slightly do not affect the image quality much [18].The purpose of singular value decomposition is to reduce a dataset containing a large number of values to a dataset containing significantly fewer values, but which still contains a large fraction of the variability present in the original data. SVD analysis results in a more compact representation of these correlations, especially with multivariate datasets and can provide insight into spatial and temporal variations exhibited in the fields of data being analyzed.

The embedding is directly related with the extraction algorithm. The embedding algorithm is basically a combination of the watermark with the chosen media, so the result is equivalent to:

$$I_W = E(I,W) \qquad (2)$$

where I is the original media, W the watermark, E is the embedding function and I_W the watermarked media. The function depends on the algorithm and the analyzed domain.

SVD is a numeric analysis of linear algebra which is used in many applications in image processing. It is used to decompose a matrix with a little truncate error according to the equation below:

$$A = USV^T \qquad (3)$$

Where A is the original matrix, U and V are orthogonal matrices with dimensions mxm and nxn respectively, S is a diagonal matrix of the Eigenvalues of A and T indicates matrix transposition. After the decomposition of the cover image the watermark is added using a scale coefficient α to get the following equation:

$$S + \alpha W = U_W S_W V^T_W \qquad (4)$$

Multiplying matrices U, V^T and S_W result in the marked image A_W:

$$A_W = US_W V^T \qquad (5)$$

This was possible due to the high stability of singular values (SV) of SVD. This method improves watermark robustness and resistance against many kinds of attacks.

The full singular value decomposition of an m-by-n matrix involves an m-by-m U, an m-by-n S, and an n-by-n V. In other words, U and V are both square and S is the same size as A. The singular value decomposition is the appropriate tool for analyzing a mapping from one vector space into another vector space, possibly with a different dimension.

2.6 Proposed Technique

The section describes the proposed watermarking scheme which is carried out in two phases, the watermark embedding phase and the watermark extraction phase. The watermark embedding scheme is illustrated in Figure 2.2.

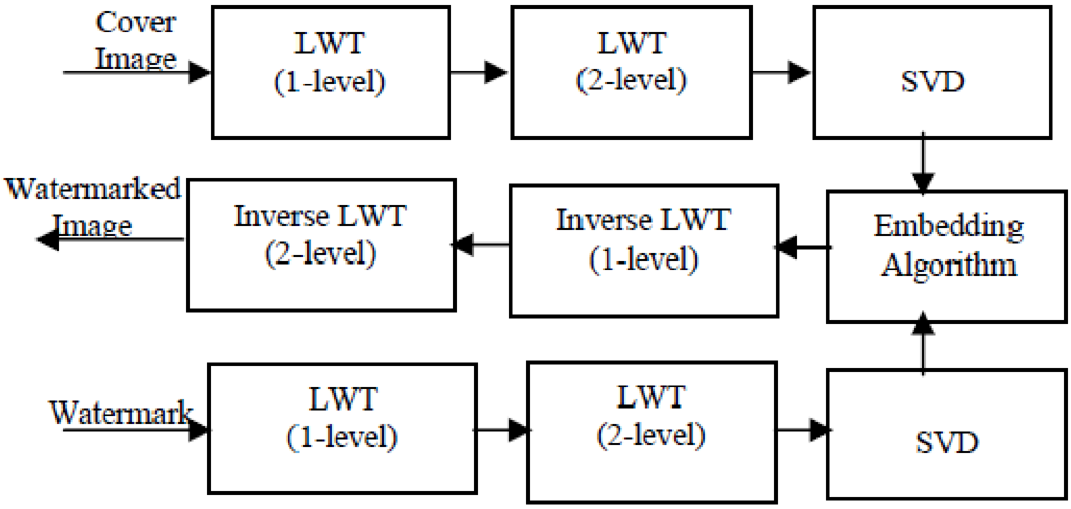

Figure 2.2: The proposed watermark embedding scheme.

The watermark extraction scheme is illustrated in Figure 2.3.

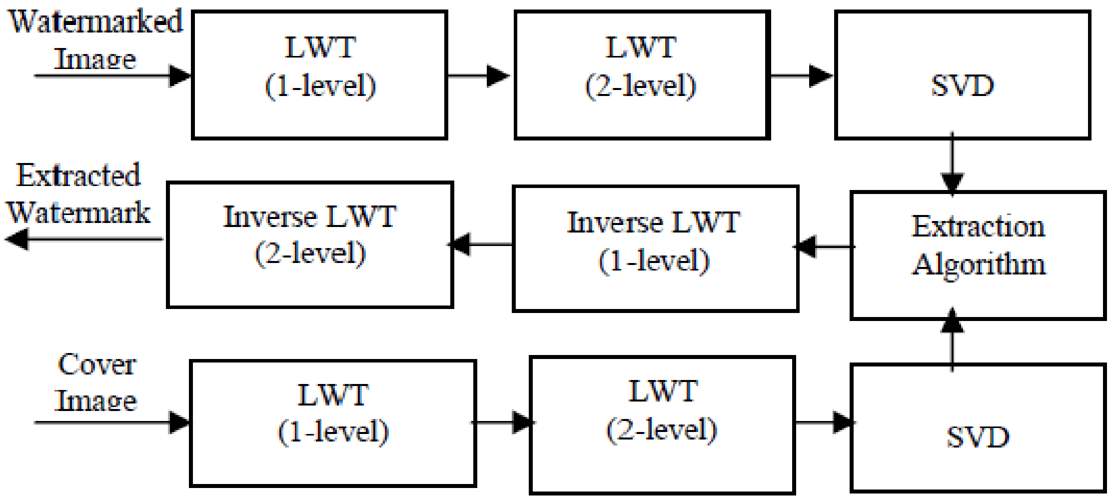

Figure 2.3: The proposed watermark extraction scheme.

2.7 Algorithm I - Watermark Embedding

Let A be the cover image, B be the watermark and k the embedding coefficient then watermarked image I is obtained by the function I= WaterMark_Embed(A,B, k); as per the following algorithm. The matlab illustration for the transformation is also given.

1. Apply first level Lifting Wavelet Transform on Cover Image [ca1,ch1,cv1,cd1]=lwt2(A);
2. Apply second level Lifting Wavelet Transform on Cover Image [ca2,ch2,cv2,cd2]=lwt2(ca1);
3. Decompose to [U,S,V] by applying SVD [U,S,V]=svd(ch2);
4. Apply first level Lifting Wavelet Transform on Watermark Image [wa1,wh1,wv1,wd1]=lwt2(B);
5. Apply second level Lifting Wavelet Transform on Watermark Image [wa2,wh2,wv2,wd2]=lwt2(wa1);
6. Decompose to [P,Q,R] by applying SVD [P,Q,R]=svd(wh2);
7. Compute embedding (D=S+k*Q)
8. Decompose to [U1,D1,V1] by applying SVD. ([U1,D1,V1]=svd(D))
9. Compute Watermarked Image matrix (CA2=U*D1*V)
10. Apply first level Inverse LWT on Watermarked Cover Image ca1=ilwt2(ca2,ch2,cv2,cd2);
11. Apply second level LWT on Watermarked Cover Image I=ilwt2[ca1,ch1,cv1,cd1];
12. I=Watermarked Image

2.8. Algorithm 2 - Watermark Extraction

Let I be the watermarked image, B be the actual watermark and k the embedding coefficient then extracted watermark I’ is obtained by the function I’= Watermark_Extract(I,B,k);

as per the following algorithm. The matlab illustration for the transformations is also given.

1. Apply first level LWT on Watermarked Cover Image [ca1,ch1,cv1,cd1]=lwt2(I);
2. Apply second level LWT on Watermarked Cover Image [ca2,ch2, cv2,cd2]=lwt2(ca1);
3. Decompose to [X,Y,Z] by applying SVD. [X,Y,Z]=svd(ch2);
4. Compute inverse embedding B=(Y-S)/k;
5. Compute watermark image matrix (wh2=P*B*R;)
6. Apply Inverse LWT on Recovered Watermark (I'=ilwt2[wa2,wh2,wv2,wd2];)
7. I'= Recovered Watermark

2.9 Experimental Work and Results

2.9.1 Experimental Measurement Metrics

We have used two quality measurements to quantify the error between images namely, Peak Signal to Noise Ratio (PSNR), and Mean Structural Similarity Index Measure (MSSIM) [21].

$$PSNR = 10 \log_{10} \frac{255^2}{MSE} \text{ and,}$$

$$\text{MSE} = \frac{\sum_{i=1}^{n} (I(i) - I'(i))^2}{n}$$

Where I and I' are the original and watermarked images respectively, n is the total number of pixels. 255 refers to the maximum possible pixel value in an eight bit image. The SSIM index is a full reference metric, in other words, the measuring of image quality based on an initial uncompressed or distortion-free image as reference. SSIM is designed to improve on traditional methods like peak signal- to-noise ratio (PSNR) and mean squared error (MSE), which have proved to be inconsistent with human eye perception. SSIM is a new paradigm for quality assessment, based on the hypothesis that the HVS is highly adapted for extracting structural information. The measure of structural similarity compares local patterns of pixel intensities that have been normalized for luminance and contrast. In practice, a single overall index is sufficient enough to evaluate the overall image quality; hence a mean SSIM (MSSIM) index is used as the quality measurement metric.

$$SSIM\ (x,y) = \frac{(2\mu_x\mu_y + C_1)(2\sigma_{xy} + C_2)}{(\mu_x^{\ 2} + \mu_y^{\ 2} + C_1)(\sigma_x^{\ 2} + \sigma_y^{\ 2} + C_2)}$$

$$MSSIM\ (X,Y) = \frac{1}{M}\sum_{j=1}^{M} SSIM\ (x_j, y_j)$$

The Lena image of size 512×512 has been selected as the cover image and for the watermark the cameraman image of size 512×512 has been used.

Table 2.1: Watermarked Images And Recovered Watermarks For Various Values Of Embedding Factor(K).

<table>
<tr><td>PSNR = 38

MSSIM = 0.948538</td><td>PSNR = 52

MSSIM = 0.997063</td></tr>
<tr><td colspan="2">0.10</td></tr>
<tr><td>PSNR = 38

MSSIM = 0.94567</td><td>PSNR = 57

MSSIM = 0.99926</td></tr>
<tr><td colspan="2">0.20</td></tr>
<tr><td>PSNR = 34

MSSIM = 0.927186</td><td>PSNR = 64

MSSIM = 0.999873</td></tr>
<tr><td colspan="2">0.5</td></tr>
<tr><td>PSNR = 30

MSSIM = 0.878370</td><td>PSNR = 60

MSSIM = 0.999881</td></tr>
<tr><td colspan="2">1.0</td></tr>
</table>

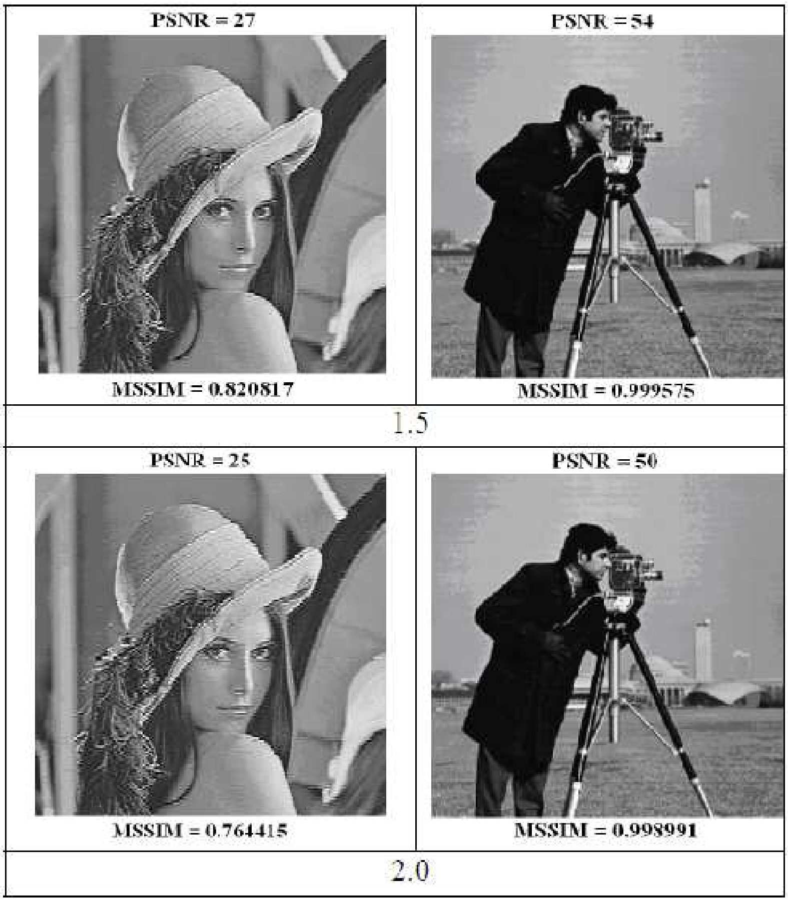

Table 2.2: List And Summary Of Attacks Simulated On The watermarked Image.

Attack /Transform	Options	Survives the attack
Cropping	% of original image: 1, 2	YES
Histogram Equalization		YES
Median Filtering	Filter size 3 × 3	YES
Salt n pepper	Filter size 3 × 3	YES
Sharpening	Filter size 3 × 3	YES
Scaling	Default value for number of levels is 64	YES
Weiner Filtering	Noise density: 0.02 to 0.05	YES
Gaussian noise	Gaussian white noise of mean 0 and variance 0.01	YES
JPEG Compression	Compression ratio: 30, , 50, 70, 90	YES

2.9.2 Results

Table 2.1 gives a pictorial representation of the effect of varying the embedding factor on the PSNR and the recovered watermarks. To test the robustness of the technique, the results in the present study were tested against the attacks listed in Table 2.2 whereas Table 2.3 shows the extracted watermarks after the watermarked image was subjected to the above mentioned attacks. The technique was also tested against JPEG compression with different quality factors i.e. different compression ratios. Table 2.4 shows recovered watermarks after simulation of JPEG Compression for different compression ratios.

Table 2.3: Watermarked Images And Recovered Watermarks After Simulation Of Various Processing Attacks On The Watermarked Image.

	PSNR = 50  MSSIM = 0.995937
Cropping	
	PSNR = 27  MSSIM = 0.739606
Histogram Equalization	
	PSNR = 26  MSSIM = 0.611905
Gaussian Noise	
	PSNR = 29  MSSIM = 0.765780
Salt and Pepper Noise	
	PSNR = 29  MSSIM = 0.840751
Median Filtering	

	PSNR = 32  MSSIM = 0.929151
Weiner Filtering	

Table 2.4: Recovered Watermarks After Simulation Of Jpeg Compression Attack For Different Compression Ratios.

PSNR = 57  MSSIM = 0.999306	PSNR = 51  MSSIM = 0.997820
Compression= 90 %	Compression=70%
PSNR = 44  MSSIM = 0.991676	PSNR = 53  MSSIM = 0.998113
Compression=50%	Compression=30%

2.9.3 Effect Of Using Different Wavelets

The lifting wavelet transform was implemented using different wavelet families and their corresponding effect on the watermarked image was observed. While Figure 2.4 presents a graphical overview of the results obtained, Table 2.5 depicts the same results in an analytical manner. Some wavelets show better performance than others. After testing the technique with wavelet families like db1, bior1.1, rbio 5.5 and rbio1.1, it was observed that rbio 5.5 wavelets shows higher performance than others for lower embedding capacity. But when capacity was increased and tested rbio1.1 shows a better performance. Hence, we have used rbio 1.1 as the wavelet in lifting scheme as these are compactly supported biorthogonal spline wavelets for which symmetry and exact reconstruction are possible with FIR filters as the filters used for decomposition and reconstruction are different, thus reducing the interference and providing better reconstruction.

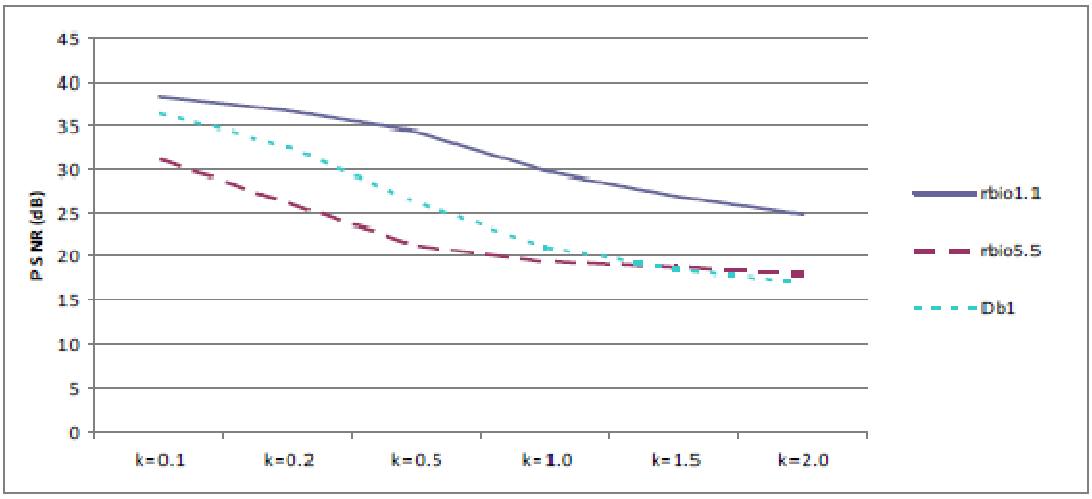

Figure 2.4: Graphical representation of embedding factor (k) versus PSNR for various wavelet families.

Table2.5: The Effect Of Various Wavelet Families On PSNR Of The Watermarked Image.

k	rbio1.1(in dB)	rbio5.5(in dB)	Db1(in dB)
0.1	38	31	36
0.2	36	26	32
0.5	34	21	26
1.0	29	19	21
1.5	26	18	18
2.0	24	18	17

2.9.4 The Gain Factor Effect

The watermark is embedded into the cover image using different embedding factors (k). In the embedding process, the singular component are multiplied by a gain factor, and then embedded in the host image coefficients. Therefore, changing the value of the gain factor has an obvious effect on both, the watermarked image, and the watermark extracted from it. The results in the proposed technique were tested for values of k in the range of 0.10 to 2.0. Table 2.1 shows the effect of changing the gain factor on the Peak Signal-To-Noise Ratio (PSNR) of the watermarked images and the recovered images. Figure 2.5 represents the same effect for the rbio1.1 wavelet being used in the current approach.

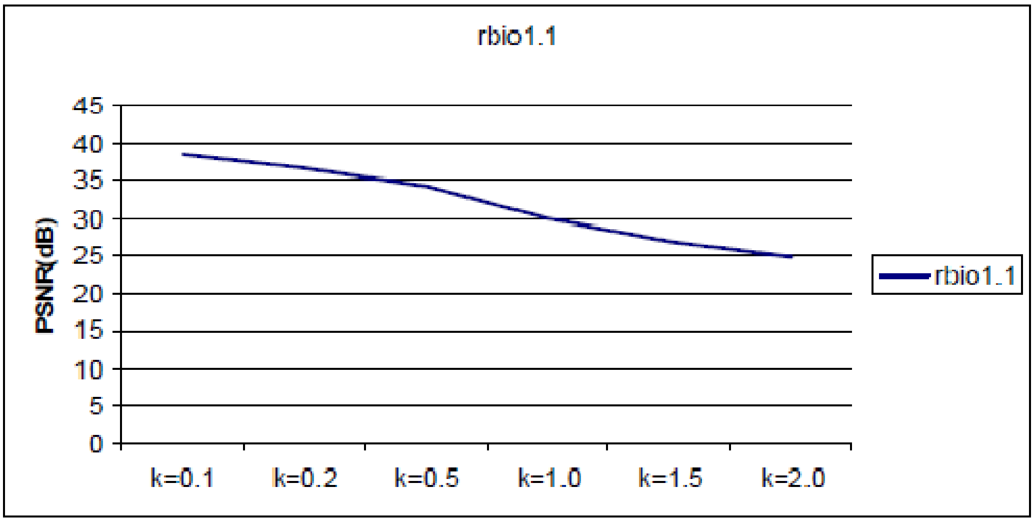

Figure 2.5: Graphical representation of embedding factor (k) versus PSNR

2.9.5 The Decomposition Level Effect

In order to embed the watermark into the host image, one should perform LWT to the host image and obtain the required coefficients for embedding. The coefficients needed for embedding can be obtained from one level (scale) of LWT or more. In this study, we perform tests that include one-level LWT, and other tests that include two-level LWT.

To show the effect of the level, a gain factor of 0.2 was selected in embedding and the tests were performed on Lena image and the watermark. The effect of the decomposition level is shown in Table 2.6. The table shows the results of two tests, the first test embeds in the approximation subband of the first level decomposition, and the second embeds in the approximation sub-band (second level) that is obtained from the first level decomposition.

It has been observed that embedding in 1st level results in a lesser value of the quality metrics as the recovered watermark is not very clear whereas in case of 2nd level, the watermarked image as well as the recovered watermark has higher value for both the quality metrics i.e. PSNR and MSSIM.

The results in the present study were tested against the attacks listed in Table 2.3, to test the robustness of the technique.

Table 2.6: Effect Of Varying The Level Of Decomposition

LWT Level	Watermarked Image		Recovered Watermark	
	PSNR	MSSIM	PSNR	MSSIM
Level 1	36	0.9381	40	0.9819
Level 2	38	0.9456	56	0.9992

2.10 Conclusion

The difference expansion watermarking methods usually embed the data bit by bit into the cover image. We have proposed an algorithm to embed bytes directly into the difference as watermark. We have analyzed the performance of various wavelets for a given capacity and we have also studied how embedding capacity varies for a given image using various wavelet decompositions by varying the payload. Some wavelets, though they seem to perform better at lower capacity, they are not able to embed like rbio1.1 smoothly at different embedding rates.

Chapter 3

An Intelligent Recursive Algorithm for Impulse Noise Removal using Lifting Scheme

3.1 Introduction

Real world signals usually contain departures from the ideal signal that would be produced by our model of the signal production process. Such departures are referred to as *noise*. Noise arises as a result of unmodelled or unmodellable processes going on in the production and capture of the real signal. It is not part of the ideal signal and may be caused by a wide range of sources, *e.g.* variations in the detector sensitivity, environmental variations, the discrete nature of radiation, transmission or quantization errors, *etc.* It is also possible to treat irrelevant scene details as if they are image noise (*e.g.* surface reflectance textures). The characteristics of noise depend on its source, as does the operator which best reduces its effects.

Many image processing packages contain operators to artificially add noise to an image. Deliberately corrupting an image with noise allows us to test the resistance of an image processing operator to noise and assess the performance of various noise filters.

Noise can generally be grouped into two classes:

- independent noise.
- noise which is dependent on the image data.

Image independent noise can often be described by an additive noise model, where the recorded image h*(i,j)* is the sum of the *true* image *f(i,j)* and the noise *n(i,j)*:

$$h(i,j) = f(i,j) + n(i,j) \qquad (1)$$

The noise *n(i,j)* is often *zero-mean* and described by its variance σ_n^2. The impact of the noise on the image is often described by the *signal to noise ratio* (SNR), which is given by

$$SNR = \frac{\sigma_s}{\sigma_n} = \sqrt{\frac{\sigma_f^2}{\sigma_n^2} - 1} \qquad (2)$$

where σ_s^2 and σ_f^2 are the variances of the true image and the recorded image, respectively.

In many cases, additive noise is evenly distributed over the frequency domain (*i.e. white noise*), whereas an image contains mostly low frequency information. Hence, the noise is dominant for high frequencies and its effects can be reduced using some kind of lowpass filter. This can be done either with a frequency filter or with a spatial filter. (Often a spatial filter is preferable, as it is computationally less expensive than a frequency filter.)

In the second case of *data-dependent noise* (*e.g.* arising when monochromatic radiation is scattered from a surface whose roughness is of the order of a wavelength, causing wave interference which results in image *speckle*), it is possible to model noise with a multiplicative, or non-linear, model. These models are mathematically more complicated; hence, if possible, the noise is assumed to be data independent.

3.1.1 Detector Noise

One kind of noise which occurs in all recorded images to a certain extent is *detector noise*. This kind of noise is due to the discrete nature of radiation, *i.e.* the fact that each imaging system is recording an image by counting photons. Allowing some assumptions (which are valid for many applications) this noise can be modeled with an independent, additive model, where the noise *n(i,j)* has a zero-mean Gaussian distribution described by its standard deviation (σ), or variance. (The 1-D Gaussian distribution has the form shown in Figure 3.1.) This means that each pixel in the noisy image is the sum of the true pixel value and a random, Gaussian distributed noise value.

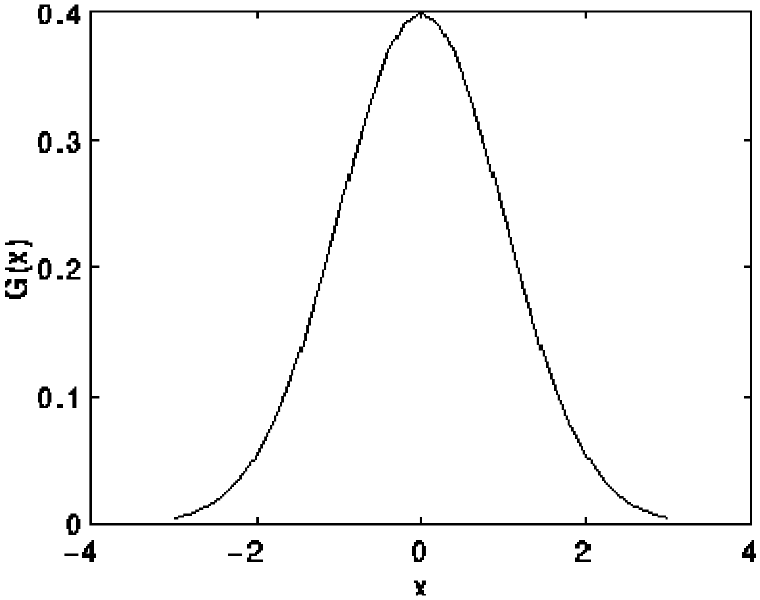

Figure 3.1: 1-D Gaussian distribution with mean 0 and standard deviation 1[55]

3.1.2 Salt and Pepper Noise

Another common form of noise is *data drop-out* noise (commonly referred to as *intensity spikes*, *speckle* or *salt and pepper noise*). Here, the noise is caused by errors in the data transmission. The corrupted pixels are either set to the maximum value (which looks like snow in the image) or have single bits flipped over. In some cases, single pixels are set alternatively to zero or to the maximum value, giving the image a `salt and pepper' like appearance. Unaffected pixels always remain unchanged. The noise is usually quantified by the percentage of pixels which are corrupted.

An Intelligent Recursive Algorithm (IRA) based on lifting filter that can efficiently remove salt and pepper noise is presented in this thesis. The algorithm does not need any threshold parameters unlike the algorithms developed so far using PSM and median based filters. It is found from the results that the proposed IRA for noise removal demonstrates much better results with lesser computation time when compared to other existing algorithms. The proposed algorithm even works for binary images corrupted with impulse noise. The image restored using the proposed algorithm is compared with restoration using median based filters. It can be observed that the visual quality is much better and the finer details are very well maintained using the proposed algorithm for both binary and grayscale images.

Noise should be removed while keeping the fine details of the image intact. An intelligent recursive noise removal algorithm (IRA) based on the lifting filter that can efficiently remove noise is presented in this paper. The algorithm does not need any threshold parameters unlike the algorithms developed so far and it demonstrates superior results in lesser computation time.

Median filter is a well known method that can remove salt and pepper noise from images. Its disadvantage is the distortion of corners and thin lines in the image. Center Weighted Median (CWM) is a superior enhancement to Median filter [46]. The center is given more weight compared to the surrounding neighbors. This filter can retain fine details of the image. Progressive Switching Median Based Filter (PSMF) has been proposed by Zhou Wang and David Zhang in [44], for the removal of impulse noise from highly corrupted images. The Center Weighted Median filter gave more importance to current pixel, preserving good image details, but offered less noise suppression when the center pixel itself is corrupted [45]. Most of the recent impulse filters [46, 47] provide good outputs at smaller noise levels and find difficulty in restoring highly corrupted images. Total Variation regularization has been used in [50] for deconvolution with salt and pepper noise. The algorithms [53, 54] are new developments in the image restoration domain.

Second generation wavelets developed by Swelden [48] have been efficiently used for many applications of image processing. The lifting scheme has been earlier applied to the progressive image sampling as seen in [42]. Adaptive versions of the Lifting Scheme have been used in areas of image reconstruction and image compression as seen in [51-52].

The idea of noise cancellation using lifting filters is not new, and recently, it has been investigated in [43]. This implementation involved numerous iterations bringing down the computational efficiency and had a shortcoming, that it needed a threshold parameter to be set every time it was run and moreover it could not work well for binary images. Similar shortcomings were observed in Progressive Switching Median Filter [44]. The threshold is determined by these algorithms by conducting numerous experimental runs. Hence, to solve these issues we propose our algorithm which intelligently determines the threshold parameter and works well for binary images as well. The Intelligent Recursive Algorithm first calculates the detail coefficients for the entire image and then intelligently determines the threshold to get the best possible results.

Moreover there is a difference in removing impulse noise in grayscale and binary images. The difficulty in removing salt and pepper noise from binary image is due to the fact that image data as well as the noise share the same small set of values (either 0 or 255) which complicates the process of detecting and removing the noise. This is different from grayscale images where salt and pepper noise could be distinguished as pixels having big difference in the amplitude compared with their neighborhood pixels. A new method was proposed in [49] specifically for binary images of engineering drawings. Hence, we have incorporated a new method to classify such pixels as *'good but marked noisy'* pixels.

3.2 Image Model

Consider an original image *f* and a noisy and degraded image *h*. The image *h* is corrupted with homogeneous impulse noise *n* which is spread equally throughput the image. So, in the usual sense any standard Image Restoration Model is given by equation (1) above.

Data from images, are highly correlated, and contain redundancy. This structure is exploited by the wavelets to represent such data accurately with a few parameters. The computations involved in obtaining this representation are fast and efficient, and linear in complexity. Because of this property, wavelets find its application in geometric modeling, data transmission, data compression, as well as in numerical computations.

Second generation wavelets developed in [48],[56],[59-71] have been efficiently used for many applications of image processing. Generating set of most significant samples for image restoration and then using them to generate an image is a highly non-linear and computationally expensive task.

The lifting scheme [42] can be viewed as a process of taking an existing wavelet and modifying it by adding linear combinations of the scaling function at the same level of resolution. The scheme consists of three steps: *Split*, *Predict* and *Update*.

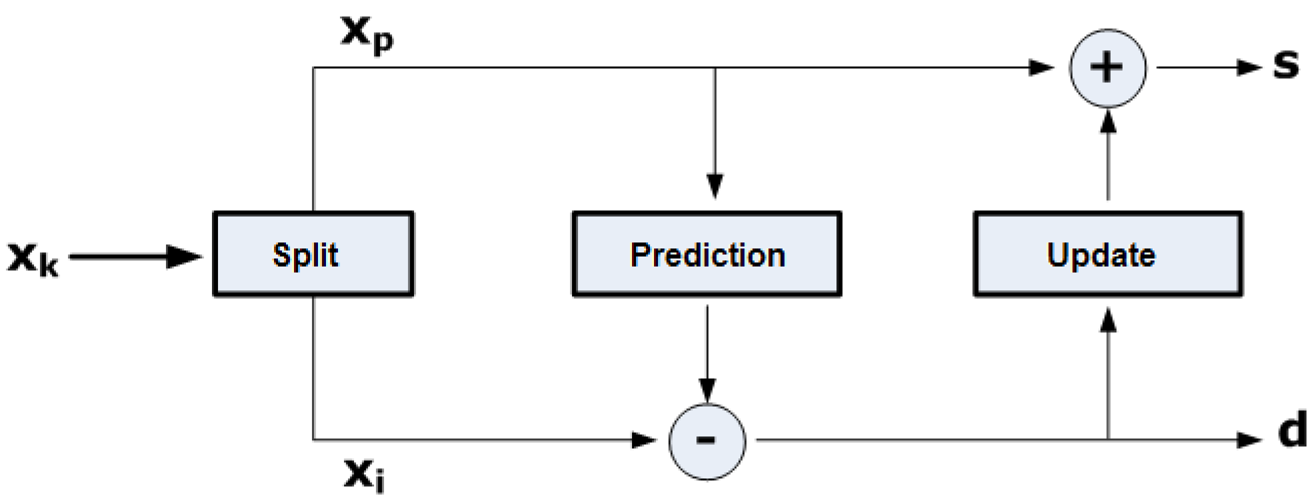

Figure 3.2: Lifting scheme[51]

In Figure 3.2, there are three basic operations: split, predict and update. In split stage the input x_k is separated into odd (x_i) and even (x_p) samples, so that each of these variables contains

half the number of samples of x_k. In the prediction stage, even samples are used to predict the odd samples. The details coefficients or high frequency (h) are calculated as prediction errors of the odd samples through the use of the prediction operator P:

$$h = x_i - P(x_p) \qquad (3)$$

To create the low frequency samples s, the even samples are updated through the update operator U:

$$s = x_p - U(d) \qquad (4)$$

3.3 Proposed Intelligent Recursive Scheme

Figure 3.3 illustrates the general structure of the proposed intelligent recursive scheme.

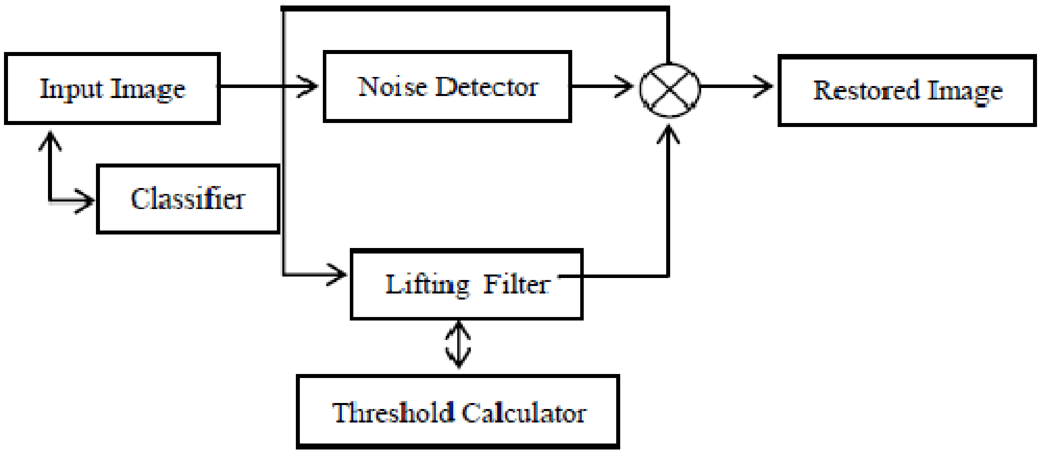

Figure 3.3: General framework of the intelligent recursive algorithm based on lifting filter

Similar to other impulse detection algorithms [43] and [44], our impulse filter is developed by prior information on natural images, i.e., a noise-free image should be locally smoothly varying, and is separated by edges. The noise considered by this detection algorithm is only salt and pepper impulsive noise which means:

a. only a portion of the image pixels are corrupted while other pixels are noise- free.
b. a noise pixel takes either a very large value as a positive impulse or a very all value as a negative impulse.

To implement the PSM or the median filter method we need to set some parameters and a threshold value. This threshold value is dependent on the image and the noise density. So, to restore different images we need to check for a range of threshold values and find out the best one. So, in our proposed algorithm we removed the need to define a threshold value. The algorithm is intelligent and determines the threshold automatically.

3.3.1 Proposed Intelligent Recursive Algorithm (IRA)

Input – Noisy Image h

Step 1: Select the first pixel X(i,j)= h(i,j)

for every pixel repeat steps from 2 to 7

Step 2: Select window size w (e.g. w= 3)

Step 3: Check if X(i,j) is an Impulse pixel then goto step 7

Step 4: Compute $\Delta i,j$ = { h(i1,j1) | i-(w-1)/2 ≤ i1 ≤ i+(w-1)/2, j-(w-1)/2 ≤ j1 ≤ j+(w-1)/2}

b=no. of black pixels in the window

w=no. of white pixels in the window

Step 5: If $\Delta i,j \neq$ NULL

Compute mean. p(i,j) = mean($\Delta i,j$)

Compute detail coefficient d(i,j) = | h(i,j) – p(i,j) |

else Increase window size till maximum [if (w < wmax) w=w+2 goto step 4]

else

if (b>w) h(i,j)=0 else h(i,j)=255

Step 6: Goto next pixel step 1

Step 7: Calculate threshold t, from detailed coefficient matrix d

for every pixel

Step 8: Check if detail coefficient is greater than threshold [If (d(i,j)>t) h(i,j)=p(i,j)]

Output : Denoised Image

The threshold parameter is calculated using the detailed coefficient matrix. The detailed coefficient d(i,j) is calculated by calculating the absolute difference between the current pixel h(i,j) value and the mean of good pixels (around the current pixel) p(i,j). Now the algorithm intelligently decides that the threshold is:

$$t = \min(d(i, j)) \qquad (2)$$

In the proposed algorithm a binary image is taken and for every pixel we count the number of good pixels around that pixel taking a window size of w=3. Now, if there are no good pixels found in this window, the algorithm because of being adaptive increases the window size to 5. Once again if no good pixels are found, then the algorithm counts the number of black (pixel value 0) and white (pixel value 255) pixels around the current pixel. The current pixel value h(i,j) is replaced by the value whichever is found greater which gives us the restored image.

3.4 Experimental Work and Results

Experimental results on the image of Lena have been presented to show the efficiency of the method. The proposed algorithm was implemented in Matlab v7.6. For evaluating the performance of the proposed algorithm, the computed results are compared by visual quality subjectively and by improvement in PSNR.

3.4.1 Measurement Metrics

PSNR for an MxN image is defined as:

$$PSNR = 20\ log_{10}\left(\frac{255}{RMSE}\right) \qquad (3)$$

where RMSE is:

$$RMSE = \sqrt{\frac{1}{MN}\sum_{i=1}^{M}\sum_{j=1}^{N}[I(i,j) - I'(i,j)]^2} \qquad (4)$$

Here i,j is the pixel position, I is the original image and I' is the restored image.

3.4.2 Results and Discussion

The experimental results show the wide applicability of the method for de-noising grayscale and binary images corrupted with all levels of noise densities. For 10%, 20% and 50% homogeneous salt and pepper noise a single iteration was found sufficient for the image restoration. The quality of the restored image at 50% is almost similar to the original image (as in Figure 3.4). In [43] and [44] more than one iteration was required to de-noise the image at 50% noise levels. Figure 3.5 shows that, for 80% homogeneous salt and pepper noise two iterations were sufficient for generating the results, while [43] required three iterations for the same level of noise. Even at highly corrupted image at 95% homogeneous salt and pepper noise four iterations were found sufficient for generating the results shown at Figure 3.6. At only 5% signal level the median based filters could not restore the image even after many iterations. In each case the threshold parameters were automatically calculated and the time complexity was found to be a lot lesser.

Figure 3.4: Image Restoration using proposed algorithm for 50% noise

(a) Original Lena

(b) Lena with 50% Salt and Pepper Noise

(c) Restored Image by proposed algorithm – 1st Iteration

(d) Restored Image by Median Filter 1st Iteration

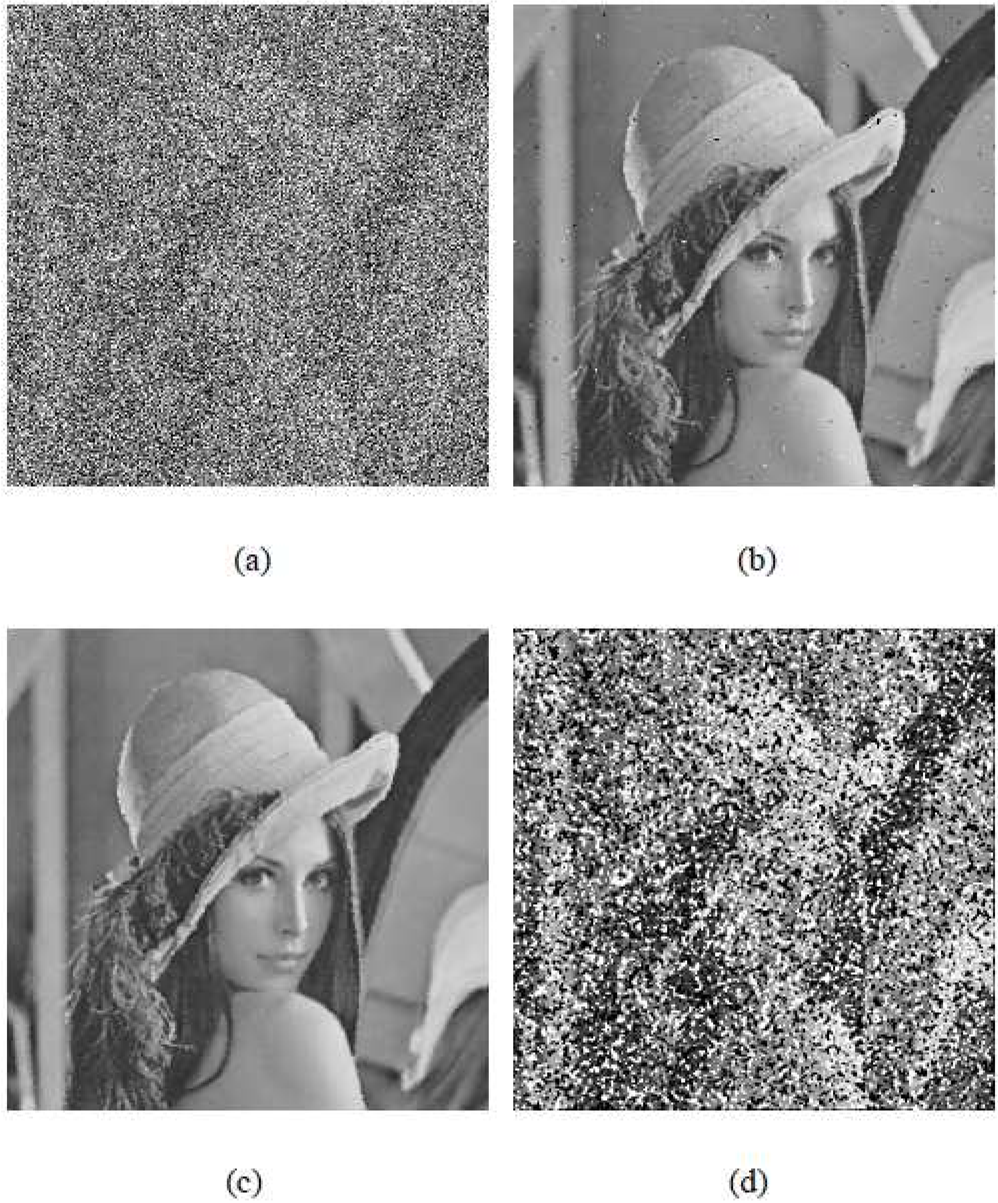

Figure 3.5: Image Restoration using proposed algorithm

(a) Lena with 80% Salt and Pepper Noise
(b) Restored Image by proposed algorithm – 1st Iteration
(c) Restored Image by proposed algorithm – 2nd Iteration
(d) Restored Image by Median Filter 2nd Iteration.

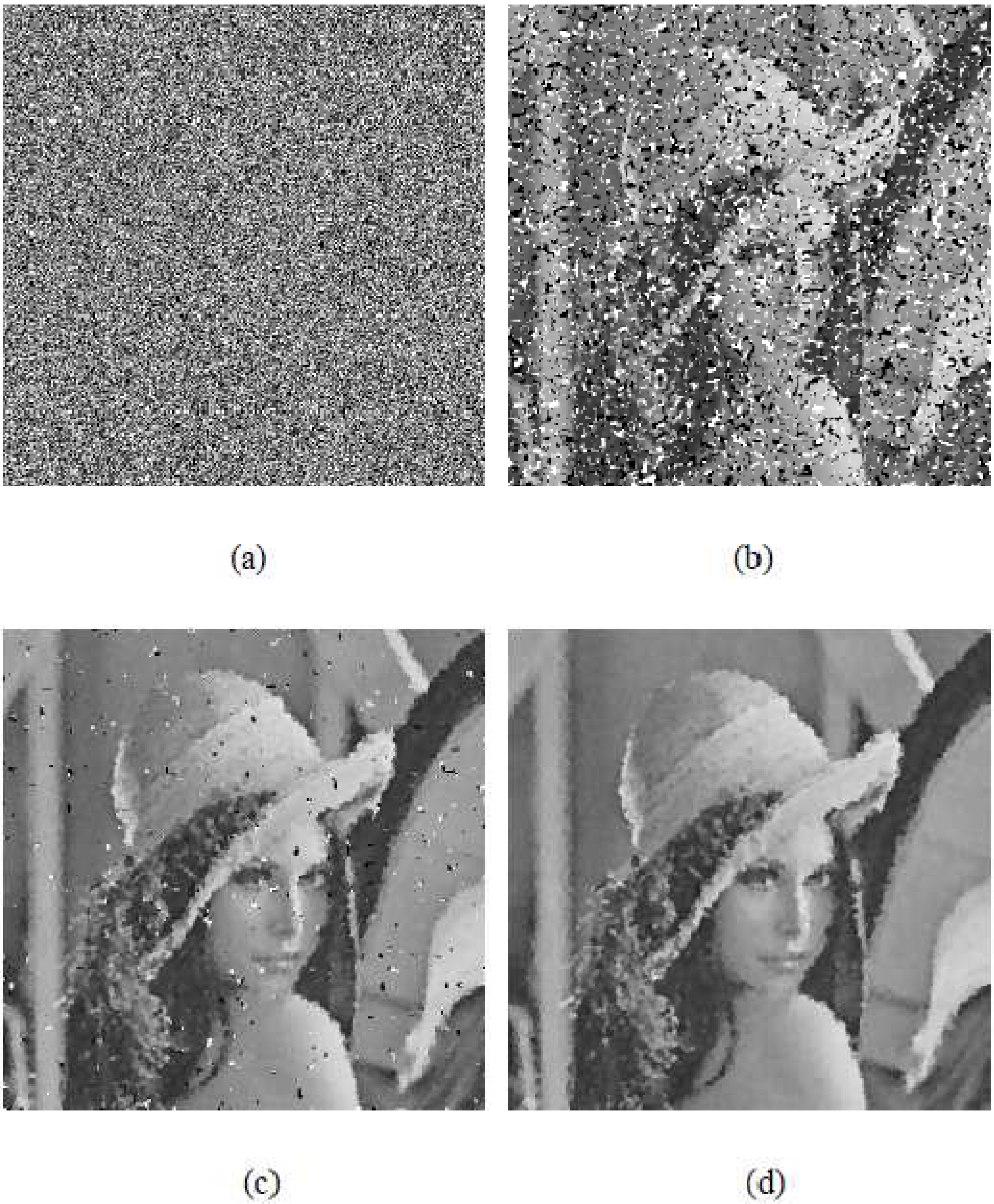

Figure 3.6: Image Restoration for highly corrupted image

(a) Lena with 95% Salt and Pepper Noise

(b) Restored Image by proposed algorithm – 1st Iteration

(c) Restored Image by proposed algorithm – 2nd Iteration

(d) Restored Image by proposed algorithm – 4th Iteration

The proposed algorithm even works for binary images corrupted with impulse noise.

Figure 3.7 shows a binary test image corrupted by 50% impulse noise. This image is restored using the proposed algorithm in one iteration and is compared with the restored image using the median filter method. It can be observed that the visual quality is much better in the image restored using the proposed algorithm.

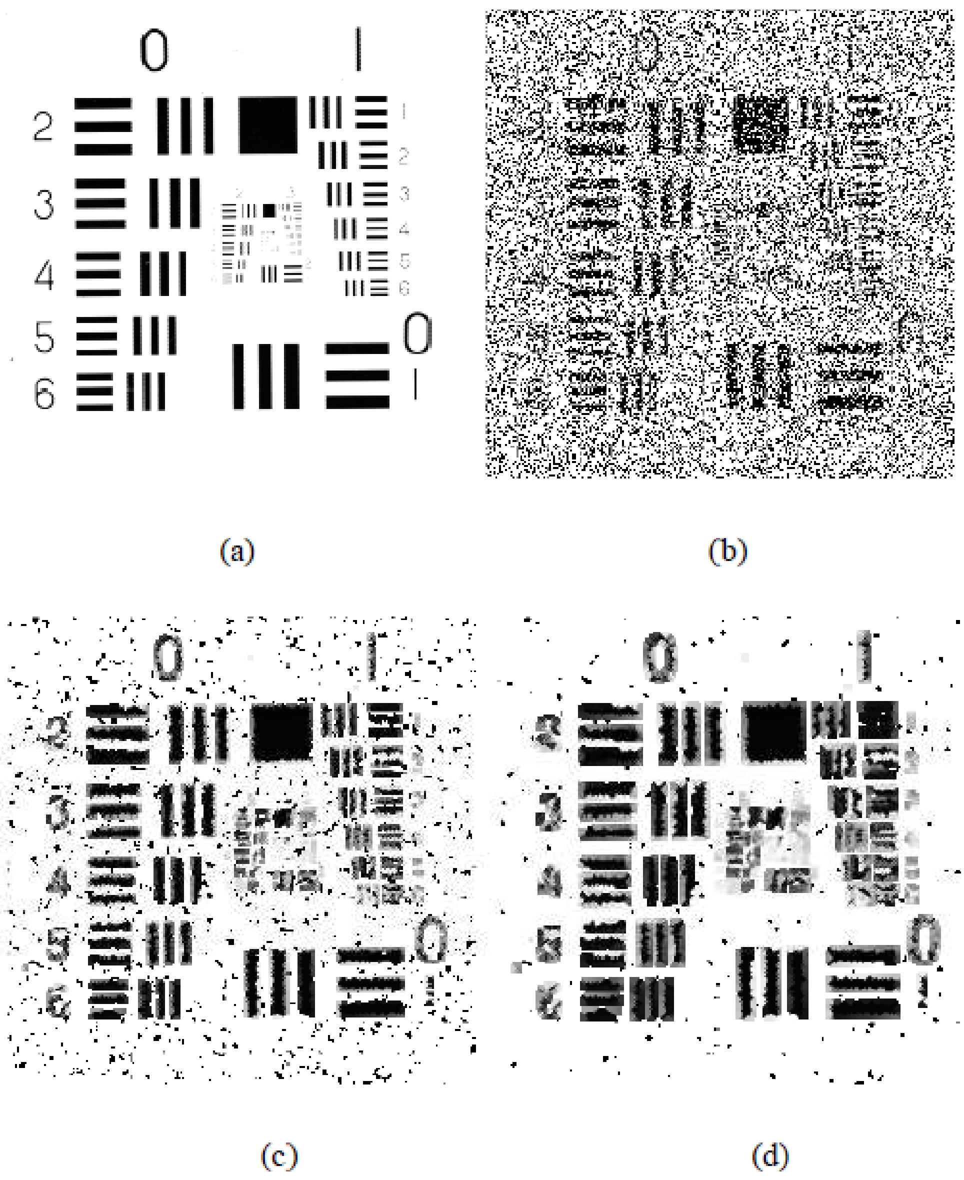

Figure 3.7: Image Restoration for Binary Images

(a) Original Binary Test Image
(b) Test Image with 50% Salt and Pepper Noise
(c) Restored Image by Median Filter
(d) Restored Image by proposed algorithm

Table 3.1 shows the performance of the proposed method with other algorithms. Our proposed algorithm shows higher PSNR values compared to the other median-based methods especially when noise ratios are high.

Table 3.1: Comparing PSNR At Different Noise Densities

Test Image	Noise Density (%)	PSNR (in dB) for PSM Filter	PSNR (in dB) for Median Filter	PSNR (in dB) for Proposed Algorithm
Lena (512 x 512)	10%	42.3	33.01	**42.95**
	20%	38.36	30.98	**39.51**
	50%	32.82	25.95	**34.22**
	80%	27.48	12.13	**29.28**

Table 3.2 shows the time complexity of the proposed method with other algorithms. Our proposed algorithm shows good time complexity compared to adaptive median- based and Edge Preservation Filter [55]

Table 3.2: Time Complexity - Comparison Of CPU Time (In Seconds)

Test Image	Noise Density	Adaptive MF	Edge PF [14]	Proposed
Lena 512x 512	70%	23	6865	**53**
	90%	311	>12000	**91**
	95%	346	>12000	**94**
Bridge 512 x 512	70%	56	8003	**54**
	90%	311	>12000	**92**

These measures hence show the superiority of our proposed algorithm using second generation wavelets and the lifting filter as compared to PSM Filter.

3.5 Conclusion

We have proposed a much improved impulse noise removal algorithm based on the lifting filter that can give us acceptable results for image restoration even at 95% degradation by noise. This algorithm also works well for binary images corrupted with impulse noise. The proposed algorithm yields better results at 10%, 20%, 50% and 80% noise densities. Moreover other median filters develop patches at very high noise densities such as 95%, but the proposed algorithm restores the image taking only 4 iterations. The increment in the PSNR values with the other filters quantifies the improvement in the algorithm. The time complexity shown in Table 3.2 proves that the algorithm is computationally takes very less time in comparison to other methods[55].

Chapter 4
Fast Progressive Image Transmission

4.1 Introduction

Progressive image transmission provides a convenient User Interface when images are transmitted slowly. We present a progressive image reconstruction scheme based on the multiscale edge representation of images. In the multiscale edge representation, an image is decomposed into Most Significant Points (MSP) which represent the strong edges and Insignificant Points (ISP) which represent weak edges. Image reconstruction is done based on the approximation of image regarded as a function, by a linear spline over adapted Delaunay triangulation. The proposed method progressively improves the quality of the reconstructed image till the desired quality is obtained.

With the emergence of the World Wide Web, images have become an important means of communicating information in the formerly textonly Internet. When people view an image through a low speed connection, for example, via a telephone line or via wireless networks, it will take much time to transmit the whole image. Even with increased bandwidth, transmitting large images such as pictures captured by digital cameras is still relatively slow. The desire to let mobile users participate in the Internet leads to the need to cope with even narrower bandwidth and smaller client displays. If the delay is too long user will feel irritated and will give up. In order to re- duce the bandwidth required for transmitting a given image in a given time, image compression techniques are commonly used to encode images. The encoded results, instead of the original images, are transmitted over the Internet. After decoding, we can obtain the decoded images, which are similar to the original ones.

Rohit Verma and Siddavatam Rajesh [22],[23],[24] have developed a fast image reconstruction algorithms using second generation wavelets and splines. Image Compression and Reconstruction algorithms have been developed by many researchers.

Siddavatam Rajesh [25] has developed a fast progressive image sampling using B-splines. Carlos Vazquez et al, [28] has proposed interactive algorithm to reconstruct an image from non-uniform samples obtained as a result of geometric transformation using filters Delaunay triangulation [34],[37] has been extensively used for generation of image from irregular data points. The image is reconstructed either by linear or cubic splines over Delaunay Triangulations of adaptively chosen set of significant points[26]. This paper concerns with progressive triangulation of an image using standard gradient edge detection techniques and reconstruction using bivariate splines from adapted Delaunay triangulation until the desired quality of the reconstructed image is not obtained.

Although image compression provides an efficient and effective method to reduce the amount of data needed to represent an image, it oftentimes requires receivers to wait for the completely encoded results before reconstructing the image. If the decoded image is not the expected one, then receivers must transmit another image again. Progressive Image Transmission (PIT) techniques have been proposed to alleviate this problem by first sending a coarse version of the original image and then resending it progressively. Progressive image transmission can help reducing the latency when transmitting raster images over low bandwidth links[27]. Often, a rough approximation (preview) of an image is sufficient for the user to decide whether or not it should be transmitted in greater detail[29],[31-33]. This allows the user to decide whether to wait for a more detailed reconstruction, or to abort the transmission. Progressive image transmission has been widely applied for many applications, such as teleconferencing, remote image database access and so on.

Existing approaches for PIT have adopted, explicitly or implicitly, the minimal distortion principle to decide the importance. For example, in the SPIHT algorithm [38], the coefficients with larger magnitude are considered more significant for they will cause larger distortion. The algorithm will therefore sort the coefficients by their magnitudes before transmission.

Some PIT techniques have adopted HVS (human visual system) weighting in spectral domain to improve the perceptual quality of the transmitted image [39],[40]. However, they did not consider the attention change in spatial domain. Popular image standards such as JPEG and JPEG2000 do support ROI coding, but they do not pro- vide any mechanism for automatic ROI definition.

The thesis describes the significant sample point selection and the modeling of the 2D images using the Linear Bivariate splines is elaborated. We also describe the reconstruction algorithm and it's complexity. The significant measures for reconstruction have been discussed. Experimental results along with comparison of the proposed method with APEL are discussed in the end.

4.2 Progressive Significant Sample Point Selection

All the progressive sampling methods take the coarse-to-fine approach—some kind of uniform sampling is applied again and again in different resolutions. The concept is adding one sample point at a time, with the key question being where the next sample should be placed. If our goal is a good reconstruction, the next sample location should be the one that minimizes the expected overall reconstruction error. This section provides a generic introduction to the basic features and concepts of novel Progressive Sample Point Selection algorithm.

4.3 Proposed Algorithm

Let M be a mXn matrix representing a grayscale image. The algorithm involves following steps:-

1) Initialization: initialization of variables.
2) Edge Detection: Edge detection using sobel and canny filters.
3) Filtering: Passing the images/matrices through range filter.
4) First Phase Transmission: Transmission of strong edges resulting in a coarse image.
5) Second Phase Transmission: Transmission of weak edges resulting in a fine image.
6) Third Phase Transmission: Detailed information for improving the reconstructed image.
7) Subsequent Phase Transmission: detailed transmission is continued till

desired resolution is achieved.

4.3.1 Initialisation

$$X1=0;\ X2=0;\ X3=0 \qquad x \in X1, X2, X3$$
$$Y1=0;\ Y2=0;\ Y3=0 \qquad y \in Y1, Y2, Y3$$
$$Z1=0;\ Z2=0;\ Z3=0 \qquad z \in Z1, Z2, Z3$$

X,Y,Z are Matrices for representing x,y,z pixel co-ordinates.
H is the starting level for third phase retransmission.
M is the increment level for third phase retransmission. The values of H and M represent the network bandwidth used for image transmission
Count1=0; Count2=0; Count3=0; are Integers representing the number of points obtained for triangulation at successive phases of transmission.
Xs is Data Set for Sobel Filter and Xc is Data Set for Canny Filter.

4.3.2 Edge Detection

An edge detector like sobel or canny takes a grayscale image as its input and returns a binary image of the same size, with 1's where the function finds edges in the original image and 0's elsewhere.

Figure 4.1: Edge Detection (Sobel)[22]

The Sobel method finds edges using the Sobel approximation to the derivative. It returns edges at those points where the gradient of I is maximum. In this method all the edges that are not stronger than a default threshold value are ignored. We can also specify our own threshold value. So this method does not identify weak edges which can be seen clearly in the Figure 4.1. This method was giving too less points to get the required triangulation.

The Canny method finds edges by looking for local maxima of the gradient of image. The gradient is calculated using the derivative of a Gaussian filter. The method uses two thresholds, to detect strong and weak edges, and includes the weak edges in the output only if they are connected to strong edges. This method is therefore more likely to detect true weak edges. The result is the following image. But again this resulted in too many points for the required triangulation.

Figure 4.2: Edge Detection (Canny)[22]

4.3.3 Filtering

After identifying the edges, the resulting image is passed through a filter so that the edges become prominent and we get more points near the edges. In order to obtain good triangulations most significant points are chosen. Range filter filters an image with respect to its local range. It returns an array, where each output pixel contains the range value (maximum value - minimum value) of the 3-by-3 neighborhood around the corresponding pixel in the input image.

4.3.4 First Phase Transmission

Input: Original Lena Image I(x,y);

Step 1: for k=1, 3, 5, 7.....................2n-1

Step 2: Locate a point P(x,y) such that P (x,y) $\in$ Xs,

Step 3: Add P(x,y) to matrices X1, Y1 , Z1

Step 4: count = count+1

Step 5: end

Output: I (X1, Y1, Z1) $\in$ Xs

4.3.5 Second Phase Transmission

Input: X=0 ; Y=0; count=0 ; Z=0; I (X, Y)

Step 1: for k= 1, 4,7,11....................3n-2

Step 2: Locate a point P(x,y) such that

Step 3: P(x,y) $\in$ Xc and P(x,y) $\notin$ Xs

Step 4: Add P(x,y) to matrices to X2, Y2 and Z2

Step 5: count = count+1

Step 6: end

Output: I(X2, Y2, Z2) $\in$ Xc $\cup$ Xs

4.3.6 Delaunay Triangulation

Delaunay Triangulation [35, 36, 37] is also popular due to its following properties:

1) It gives a unique set of triangles T, provided that no four points in S are co-circular,

2) It guarantees optimal triangulation according to the min-max angle criterion, i.e. the smallest angle is maximal.

3) It gives the smoothest piecewise linear approximation for a given data set.

In the Delaunay triangulation method [37], the location of the global nodes defining the triangle vertices and then produce the elements by mapping global nodes to element nodes. Element definition from a given global set can be done by the method of Delaunay Triangulation. The discretization domain is divided into polygons, subject to the condition that each polygon contains only on global node, and the distance of an arbitrary point inside a polygon from the native global node is smaller than the distance from any other node. The sides of the polygon thus produced are perpendicular bisectors of the straight segments connecting pairs of nodes.

4.3.7 Third Phase Transmission

To further improve the triangulations, in every triangle a point is inserted at the centroid of the triangle and triangles are formed including that point. This algorithm is useful for even those images having low gradient at the edges or weak edges.

Input: TRI(X1+X2, Y1+Y2)

```
Step 1:   T=Dataset (TRI)
Step 2: for threshold=H to 0 step M
Step 3:          for m=1, 2, 3,  4,5,6,7...................................N
Step 4:             If  Area  > Threshold
Step 5:                   C(x,y)=Centroid of Triangle TN
Step 6:                           add C(x,y) to data set (X3,Y3,Z3)
Step 7:                   count = count+1
Step 8:             end
Step 9:   end
```

Step 10 : TRI = delaunay(X,Y)

Output: I(X3, Y3, Z3) $\in$ Xc $\cup$ Xs

4.3.8 Subsequent Phase Transmission

Depending upon the requirement of resolution the image fine detail information can be generated further by centroid of triangles and passed in subsequent phases till required resolution is obtained.

4.4 Image Reconstruction Using Linear Bivariate Splines

The transmitted image as a result of the three phases of transmission is reconstructed at the receiver's end. The reconstruction is carried out based on the approximation of image regarded as a function, by a linear bivariate spline over adapted Delaunay triangulation.

The Linear Bivariate Splines are used very recently by Laurent Demaret et al [9]. The image is viewed as a sum of linear bivariate splines over the Delaunay triangulation of a small recursively chosen non uniform set of significant samples Sk from a total set of samples in an image denoted as Sn. The linear spline is bivariate and continuous function which can be evaluated at any point in the rectangular image domain in particular for non uniform set of significant samples denoted as Sk from a total set of samples in an image denoted as Sn.

If we denote Ω as the space of linear bivariate polynomials, for the above set

$S_k \subset S_n$, the linear spline space Ω_L, containing all continuous functions over the convex hull of Sk denoted as [Sk].

Definition: If for any triangle $\Delta \in T(S^k)$ where $T(S^k)$ is the delaunay triangulation of S^k is in Ω defined as

$$\Omega_L = \{x : x \in [S^k]\} \forall \Delta \in T(S^k) \mid x \in \Omega$$

then any element in Ω_L is referred to as a linear spline over $T(S_k)$. For given luminance values at the points of S, {I(y): y∈ S} there is a unique linear spline interpolant L(S, I) which gives

$$L(S,I)(y) = I(y) \forall \ y \in S$$

where I(y) denotes the image I with y samples that belong to S. Using the above bivariate splines and the concept of Significant Sample point selection algorithm discussed above the original image can be approximated and the reconstruction of the image can be done as per the algorithm given below.

4.5 Reconstruction Algorithm

The following steps are used to reconstruct the original image from set of regular points comprising of significant (S_K) and insignificant points (I_K):

INPUT:

1. Let S^N=data set $S \in S^K \cup I^{K_i}$

2. Z^0: luminance

3. S^0: set of regular data for initial triangulation

Step1. Use Delaunay triangulation and Linear Bivariate Splines to produce unique set of triangles and image.

Step2. Use Progressive Significant sample point selection algorithm to find a set of new significant points (SP).

Step3. Get $S^K=S^{K-1}+SP$

Step4. Repeat steps 1 to 3 to get the image $I_R(y)$ Step5. Return S^K and $I_R(y)$

OUTPUT:

Most Significant Sample Set (S^K) and Reconstructed Image $I_R(y)$

4.6 Algorithm Complexity

In general, the complexity of the non-symmetric filter is proportional to the dimension of the filter n^2, where n * n is the size of the convolution kernel. In canny edge detection, the filter is Gaussian which is symmetric and separable. For such cases the complexity is given by n+1 [41]. All gradient based algorithms like Sobel do have complexity of O(n). The complexity of well known Delaunay algorithm in worst case is O(n^ceil(d/2)) and for well distributed point set is ~ O(n). N is number of points and d is the dimension. So in 2D, Delaunay complexity is O(N) is any case.

Step 1: Sobel Edge Detector: O(n)

Step 2: Canny Edge Detector: O(n)

Step 3: Filtering (rangefilt) : O(n)

Step 4: First Phase Transmission: O(2n-1)=O(n)

Step 5: Second Phase Transmission: O(3n-2)=O(n)

Step 6: Third Phase Transmission: O(n)

Step 7: Image Reconstruction: O(n)

Hence the total complexity of the proposed algorithm is O(n) which is quite fast and optimal.

4.7 Experimental Setup

The algorithm has been tested with MATLAB simulation on standard LENA image.

4.8 Measurement Metrics

A well-known quality measure for the evaluation of image reconstruction schemes is the Peak Signal to Noise Ratio (PSNR),

$$PSNR = 20 * \log 10\,(b / RMS)$$

where b is the largest possible value of the signal and RMS is the root mean square difference between the original and reconstructed images. PSNR is an equivalent measure to the reciprocal of the mean square error. The PSNR is expressed in dB (decibels). The popularity of PSNR as a measure of image distortion derives partly from the ease with which it may be calculated, and partly from the tractability of linear optimization problems involving squared error metrics.

4.9 Results and Discussions

We have used absolutely addressed Picture Element coding (APEL) [40] to compare the effectiveness of our proposed method. APEL is a robust, loss-less image coding technique, which transforms binary images into a tessellation of independent black picture elements. As the APEL technique operates on a binary level, the encoding of grey-scale images must employ a Bit Plane Coding (BPC) [39] stage. APEL inter-leaves and sends the larger pixels from each of the bit-planes immediately after the transmission has begun so that a coarse image can be encoded by the recipient. Subsequently, as further pixels arrive, a finer image can be decoded by the recipient. APEL decreases the visual impact of errors by rearranging the addresses of pixels in an ascending order and placing two contiguous pixels a considerable distance apart in the data-stream, the probability of both being destroyed by the same burst is de- creased. Error can be detected and removed by removing the out-of-order addresses and consecutively transmitted non-neighbor pixels.

The proposed method transmits the image pixels as per increasing order of significance. Proposed method sends the pixels corresponding to the strong edges as soon as the transmission begins and enables the recipient to reconstruct a coarse image. In due course, pixels corresponding to weaker edges and other lesser significant pixels (second and third phase transmission) are send to the recipient which improves the definition of the reconstructed image. In our proposed method we define the reconstruction error as $|| I_O - I_R || / || I_O ||$, where I_O is the original image and I_R is the reconstructed image.

The reconstructed image at various levels of transmission for APEL coding scheme and proposed method are shown in Figure 4.3.

(a) Proposed Method

(b) APEL Coding

Figure 4.3: Comparison of (b) APEL coding[19] and (a) proposed method at various levels of transmission

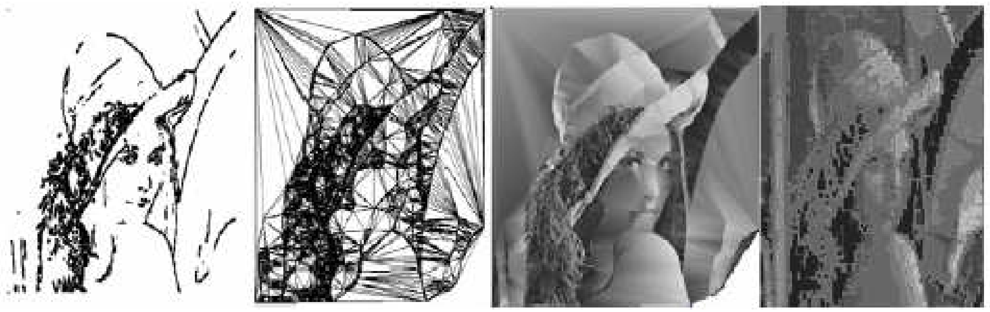

Figure 4.4a Figure 4.4b Figure 4.4c Figure 4.4d

Figure 4.4: (a)-(d)First phase Transmission

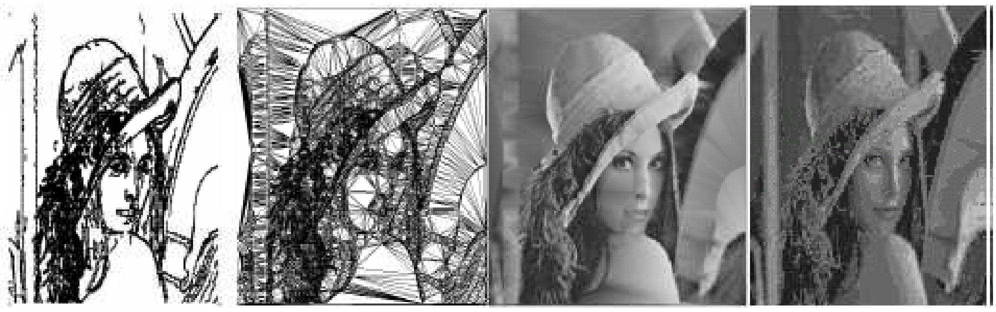

Figure 4.5a Figure 4.5b Figure 4.5c Figure 4.5d

Figure 4.5: (a)-(d) Second phase Transmission

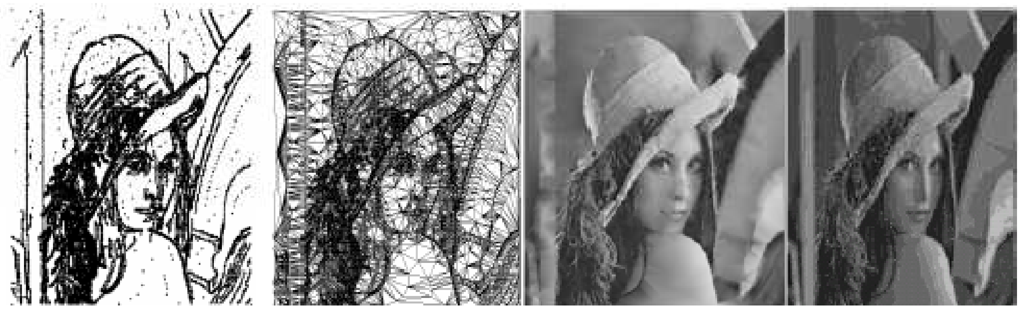

Figure 4.6a Figure 4.6b Figure 4.6c Figure 4.6d

Figure 4.6: (a)-(d) Third phase Transmission

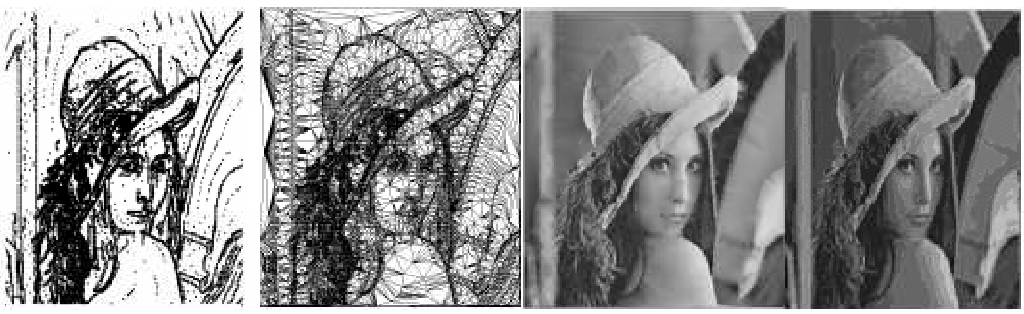

Figure 4.7a Figure 4.7b Figure 4.7c Figure 4.7d

Figure 4.7: (a)-(d) Fourth phase Transmission

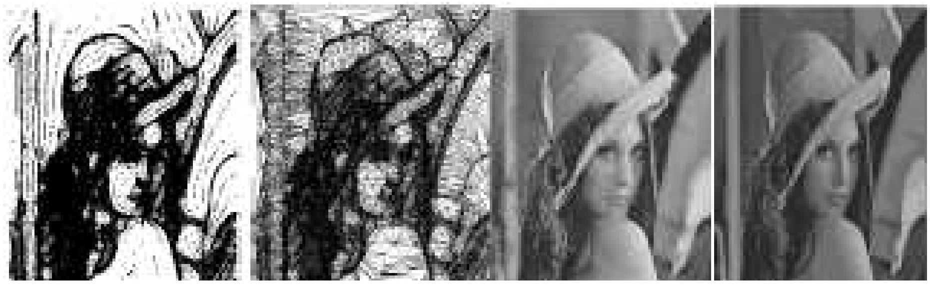

Figure 4.8a Figure 4.8b Figure 4.8c Figure 4. 8d

Figure 4.8:(a)-(d) Fifth phase Transmission

Table 4.1: PSNR at various stages of transmission

S No	Progressive Transmission Phases	Proposed Method dB
1	First phase - Figure 4.4 (a) – 4.4(d)	13.90
2	Second phase – Figure 4. 5 (a) – 4.5(d)	21.68
3	Third Phase – Figure 4.6(a) – 4.6(d)	21.97
4	Fourth Phase –Figure 4.7(a) – 4.7(d)	23.41
5	Fifth Phase – Figure 4.8(a) – 4 . 8(d)	27.22

4.10 Conclusions

In this paper, algorithm based on significant point selection is applied for progressive image transmission. Experimental results on the popular image of Lena are presented to show the reconstructed image at various phases of transmission. Set of regular points are selected using Canny and Sobel edge detection and Delaunay triangulation method is applied to create triangulated network. The set of increasingly significant sample points are transmitted in each transmission phase. The gray level of each sample point is interpolated from the luminance values of neighbor significant sample point. The original image, sample points, Delaunay triangulation and its reconstruction results along with the error image are shown for LENA image.

The PSNR value goes on increasing towards the latter phases of transmission. Thus we can fairly approximate that the proposed Progressive Transmission technique can transmit the image progressively varying the image quality. This indicated by the range of the PSNR that varies from 13.9 to 27.22 dB.

Chapter 5
Conclusions and Future Scope

5.1 Conclusion

In this thesis security based image processing using state of art mathematical concepts has been discussed. Key concepts used are given below:

1. Singular Value Decomposition
2. Discrete Fourier Transform
3. Wavelet Transform
    (a) Time frequency Analysis
    (b) Time Scale Analysis
    (c) Discrete Wavelet Transform
4. Lifting Scheme
5. Linear Bivariate Splines

A novel approach to image watermarking has been given. The watermark is embedded in the transform domain. Lifting Wavelet scheme with singular value decomposition has been proposed. The algorithm for watermark embedding has been developed. The algorithm has been experimentally evaluated. The water extraction algorithm has also been developed. The extraction algorithm has been experimentally tested. The results have been found to be very promising. The scheme for watermark embedding and extraction has also been tested against all known attacks. The watermark has survived all attacks. The scheme can therefore be construed as robust and secure.

In the thesis we also proposed an intelligent recursive algorithm for 95% salt and pepper noise removal. Lifting scheme has been used in the proposed algorithm. The algorithm has been experimentally tested for varying noise levels. Key features of the algorithm include less time complexity, intelligent threshold determination and superior operation at high noise levels.

We also propose a progressive image transmission algorithm using linear bivariate splines. The image representation is segmented in phases using progressive significant sample point selection. Coarser data using Sobel and Canny edge detector filters is generated in phase one. Finer details of weaker edges are included in subsequent phases. An image reconstruction algorithm using progressive transmission scheme has been developed. The algorithms have been experimentally tested to have resulted in superior performance.

To sum up, the main objectives of the thesis can be summarized as follows:

1. The lifting wavelet transform (LWT) and singular value decomposition (SVD) techniques for robust digital watermarking.
2. Intelligent Recursive Algorithm (IRA) based on lifting filter that can efficiently remove noise.
3. Progressive image reconstruction scheme based on the multi-scale edge representation.

Following Algorithms have been proposed.

1. Watermark Embedding using LWT and SVD

2. Watermark Extraction using LWT and SVD
3. Impulse Noise Removal
4. Progressive Image Transmission Scheme
5. Image Reconstruction Scheme

5.2 Future Scope

The watermark embedding scheme can be extended to include encrypted watermarks. Watermark extraction algorithm can be extended to perform watermark validation automatically. Suitable feature extraction and matching techniques have to be explored.

The noise removal scheme has been implemented for stationary images. This can be extended to noise removal in case of non stationary images for dynamic denoising.

In case of the progressive image transmission the schemes for optimizing the data for each phase needs to be studied. The phasewise data compression and decompression schemes need to be evaluated.

References

[1] C. I. Podilchuk and E. J. Delp, "Digital Watermarking:Algorithms and Applications," IEEE Signal Processing Magazine, pp. 33-46, July 2001

[2] I. J. Cox, M. L. Miller, and J. A. Bloom, "Digital Watermarking", Morgan Kaufmann Publishers, 2002.

[3] R. G. van Schyndel, A. Z. ltrkel and C.F.Osbome, "A Digital Watermark" IEEE, 1994.

[4] Hartung F and Kutter M, "Multimedia Watermarking Technique", IEEE Proceeding on Signal Processing", Volume 87, NO.7, pp.1079-1107, July 1999.

[5] O.G Pla, Lin E.T, and Delp E.J, "A Wavelet Watermarking Algorithm Based on a Tree Structure", Tech. Rep., Polytechnic University of Catalonia, Spain, 2004.

[6] Z Yuehua., C. Guixian and D. Yunhai, "An Image Watermark Algorithm Based on Discrete Cosine Transform Block Classifying", ACM Int. Conf., pp. 234-235, 2004.

[7] X. J. Wu, Hu. Z. Gu, and J.Huang "A Secure Semi-Fragile Watermarking for Image Authentication Based on Integer Wavelet Transform with Parameters", Tech. Rep., Sun Yat-Sen University, China, , 2005.

[8] H. C. Andrews and C.L. Patterson, "Singular Value Decomposition (SVD Image Coding," IEEE Transactions on Communications,24(4), pp. 425-432, August 1976.

[9] N. Garguir, "Comparative Performance of SVD and Adaptive cosine Transform in Coding Images," IEEE Transactions on Communications, 27(8), pp. 1230-1234, 1979.

[10] D. P. O'Leary and S. Peleg, "Digital Image Compression by Outer Product Expansion," IEEE Transactions on communications, 31(3), pp. 441-444, March 1983.

[11] J. F. Yang and C. L. Lu, "Combined Techniques of Singular Value Decomposition and Vector Quantization," IEEE Transactions on Image Processing, 4(8), pp. 1141-1146 , August 1995.

[12] P. Waldemar and T. A. Ramstad, "Hybrid KLT-SVD image Compression," 1997 IEEE International Conference on Acoustics, Speech and Signal Processing, Vol. 4, Munich, Germany, pp. 2713-2716, April 21-24, 1997.

[13] S. O. Ase, J. H. Husoy and P.Walsemar, " A Critique of SVD-Based Image Coding Systems," 1999 IEEE International Symposium on circuits and systems," Vol. 4, Orlando Fl, pp. 13-16, May 1999.

[14] V. I. Gorodetski, L. J. Popyack, V. Samoilov and V. A. Skormin, "SVD-based Approach to Transparent Embedding data into digital images," International Workshop on Mathematical Methods, Models and Architectures for Computer network Security (MMMACNS 2001), St. Petersbug, Russia, May 21-23, 2001.

[15] D. V. S. Chandra, "Digital Image Watermarking using Singular Value Decomposition," Proceedings of 45th IEEE Midwest Symposiumon circuits and Systems, Tulsa, OK, pp. 264-267, August 2002.

[16] R. Liu and T. Tan, "A SVD based Watermarking scheme for protecting rightful ownership,"IEEE Transactions on Multimedia,4(1), pp. 121-128, March 2002.

[17] B. Zhou and J. Chen, "A Geometric Distortion Resilient image Watermarking Algorithm Based on SVD," Chinese Journal of Image and Graphics, Vol. 9, pp. 506-512, April 2004.

[18] Bao, P. and Ma, X. Image Adaptive Watermarking Using Wavelet Domain Singular Value Decomposition. IEEE Transactions on Circuits

and Systems for Video Technology. Vol. 15, No. 1, pp 96-102, 2005.

[19] I. Daubechies and W. Sweldens, "Factoring Wavelet Transforms into Lifting Schemes," The Journal of Fourier Analysis and Applications, vol. 4.,pp. 247-269,1998.

[20] W. Sweldens, "The Lifting Scheme: A New Philosophy in Biorthogonal Wavelet Constructions", Proceedings of SPIE, pp.68-79, 1995.

[21] Zhou Wang, Alan C. Bovik, Hamid R. Sheikh, and Eero P. Simoncelli, "Image Quality Assessment: From Error Visibility to Structural Similarity", Ieee Transactions On Image Processing, Vol. 13, No. 4, April 2004.

[22] Verma, R., Srivastava, G.K., Mahrishi, R., Siddavatam, R. " A Fast Image Reconstruction Algorithm Using Significant Sample Point Selection and Linear Bivariate Splines." IEEE TENCON, pp. 1–6. IEEE Press, Singapore, 2009.

[23] Verma, R., Srivastava, G.K., Mahrishi, R., Siddavatam, R. " A Novel Wavelet Edge Detection Algorithm For Noisy Images." IEEE International Conference on Ultra Modern Technologies, pp. 1–8. IEEE Press, St. Petersburg, 2009.

[24] Verma, R., Srivastava, G.K., Mahrishi, R., Siddavatam, R. " A Novel Image Reconstruction Using Second Generation Wavelets." IEEE International Conference on Advances in Recent Technologies in Communication and Computing, pp. 509–513. IEEE Press, Kerala, 2009.

[25] Siddavatam, R., Sandeep, K., Mittal, R.K. " A Fast Progressive Image Sampling Using Lifting Scheme And Non-Uniform B-Splines." IEEE International Symposium on Industrial Electronics, pp. 1645–1650. IEEE Press, Spain, 2007.

[26] Eldar, Y., Lindenbaum, M., Porat, M., Zeevi, Y.Y. " The Farthest Point Strategy For Progressive Image Sampling." IEEE Trans. Image Processing

6(9), pp. 1305–1315, 1997.

[27] Arigovindan, M., Suhling, M., Hunziker, P., Unser, M. ” Variational Image Reconstruction From Arbitrarily Spaced Samples” A Fast Multiresolution Spline Solution. IEEE Trans. On Image Processing 14(4), pp. 450–460, 2005.

[28] Vazquez, C., Dubois, E., Konrad, J.” Reconstruction of Nonuniformly Sampled Images in Spline Spaces.” IEEE Trans. on Image Processing 14(6), pp. 713–724, 2005.

[29] Cohen, A., Mate, B. ” Compact Representation Of Images By Edge Adapted Multiscale Transforms.” IEEE International Conference on Image Processing, Tessaloniki, pp. 8–11, 2001.

[30] Laurent, D., Nira, D., Armin, I. ” Image Compression by Linear Splines over Adaptive Triangulations.” Signal Processing 86(4), pp. 1604–1616, 2006.

[31] Tzu-Chuen, L., Chin-Chen, C. ” A Progressive Image Transmission Technique Using Haar Wavelet Transformation.” International Journal of Innovative Computing, Information and Control 3, 6(A), pp. 1449–1461, 2007.

[32] Eldar, Y., Oppenheim, A. ” Filter Bank Reconstruction of Bandlimited Signals from Non- Uniform and Generalized Samples.” IEEE Transactions in Signal Processing 48(10), pp. 2864–2875, 2000.

[33] Aldroubi, A., Grochenig, K. ” Nonuniform Sampling and Reconstruction in Shift Invariant Spaces.” SIAM Rev. 43, pp. 585–620, 2001.

[34] Wu, J., Amaratunga, K.” Wavelet Triangulated Irregular Networks.” Int. J. Geographical In- formation Science 17(3), pp. 273–289 2003.

[35] Barber, C.B., Dobkin, D.P., Huhdanpaa, H.T. ” The Quickhull Algorithm for Convex Hulls.” ACM Transactions on Mathematical Software

22(4), pp. 469–483, 1996.

[36] Preparata, F.P., Shamos, M.I. ” Computational Geometry.” Springer, New York, 1988.

[37] Rippa, S. ”Minimal Roughness Property of the Delaunay Triangulation.” Comput. Aided Geometric Des. 7, pp. 489–497, 1990.

[38] Said, A., Pearlman, W.A.” A New, Fast, and Efficient Image Codec Based on Set Partitioning in Hierarchical Trees.” IEEE Trans. on Circuits and Systems for Video Technology 6(3), pp. 243–250, 1996.

[39] Boson, D., McConnell, K.R., Schaphorst, R. ” FAX Facsimile Technology and Applications Handbook.”, pp. 195–199, 1992.

[40] Paul, C., Bahram, H.” Progressive Robust Image Transmission.” 6th International Workshop on Systems, Signals and Image Processing. Lancaster University, UK, 1999.

[41] Neoh, H.S., Hazanchuk, A.” Adaptive Edge Detection for Real-Time Video Processing using FPGAs.” Global Signal Processing, 2004.

[42] Siddavatam Rajesh, K Sandeep and R K Mittal, “A Fast Progressive Image Sampling Using Lifting Scheme and Non-Uniform B-Splines”, Proceedings of IEEE International Symposium on Industrial Electronics ISIE -07, June 4-7, pp. 1645- 1650, Vigo, Spain, 2007.

[43] Siddavatam Rajesh and Tasha Jaywalk, “Image Noise Cancellation by Lifting Filter using Second Generation Wavelets”, Proceedings of IEEE Atom 2009, Kottayam, Kerala, India, October 27-28, 2009.

[44] Zhou Wang and David Zhan, “Progressive Switching Median Filter for the Removal of Impulse Noise from Highly Corrupted Images”, IEEE Transactions on Circuits And Systems—II:Analog And Digital Signal Processing, Vol. 46, No. 1, January 1999.

[45] T. Chen and H.Wu, "Adaptive Impulse Detection using Center

Weighted Median Filters", Signal Processing Lett., vol. 8, no. 1, pp.1-3, Jan. 2001.

[46] Vladimir Crnojevic´, Vojin Senk and Zeljen Trpovski, "Advanced Impulse Detection based on Pixel-wise MAD", IEEE Signal Processing Letters, Vol. 11, No. 7, July 2004.

[47] Xiaoyin Xu, Eric L. Miller, Dongbin Chen and Mansoor Sarhadi, "Adaptive two-pass Rank Order Filter to Remove Impulse Noise in highly Corrupted Images", IEEE Transactions on Image Processing, Vol. 13, No. 2, February 2004.

[48] W.Swelden., "The Lifting scheme " A custom design construction of biorthogonal wavelets", Appl. Comput. Harmon. Anal., 3(2), pp.186-200, 1996.

[49] Hasan S. M. Al-Khaffaf, Abdullah Z. Talib, Rosalina Abdul Salam, "Removing Salt-and-Pepper Noise from Binary Images of Engineering Drawings", in IEEE Signal Process. Lett., vol. 11, no. 2, pp. 243–246, Feb. 2004.

[50] Brendt Wohlberg and Paul Rodriguez, "An l^1-TV Algorithm for Deconvolution with Salt and Pepper Noise", IEEE International Conference on Acoustics, Speech and Signal Processing, ICASSP 2009, pp. 1257 – 1260, 19-24 April 2009.

[51] Gemma Piella and Henk J.A.M. Heijmans, "An Adaptive Update Lifting Scheme With Perfect Reconstruction", Proceedings of International Conference on Image Processing 2001, Volume 3, pp. 190 - 193, 7-10 Oct. 2001.

[52] Weisheng Dong, Guangming Shi, and Jizheng Xu, "Signal-Adapted Directional Lifting Scheme for Image Compression", IEEE International Symposium on Circuits and Systems, ISCAS 2008, pp. 1392 – 1395, 18-21 May 2008.

[53] Bosco.A, Mancuso.M, Battiato.S, Spampinato. G, "Temporal noise

reduction of Bayer matrixed video data", IEEE International Conference on Multimedia and Expo Volume 1, pp. 681 - 684, 26-29 Aug. 2002.

[54] Fujiki, A,Matsushita.J,Imai.T, Muneyasu.M, "Technique for mixed noise reduction based on support vector machine [image denoising]" Nonlinear Signal and Image Processing, 2005. Abstracts. IEEE-Eurasip, pp. 25, 18-20 May 2005.

[55] Raymond H. Chan, Chung-Wa Ho, and Mila Nikolova, "Salt-and-Pepper Noise Removal by Median-Type Noise Detectors and Detail-Preserving Regularization", IEEE Transactions On Image Processing, Vol. 14, No. 10, pp.1479-1485, October 2005.

[56] http://homepages.inf.ed.ac.uk/rbf/HIPR2/noise.htm

[57] A. Bruce, D. Donoho, and Hong-Ye Gao. "Wavelet Analysis." IEEE Spectrum, 33(10), pp. 26–35, October 1996.

[58] J.W. Cooley and J.W. Tukey. "An algorithm for the machine calculation of complex fourier series." Mathematics of Computation, 19, pp. 297–301, 1965.

[59] L. Debnath. "Wavelets and Signal Processing." Birkhauser Boston, 2003.

[60] F. Fernandes. "Directional, Shift-Insensitive, Complex wavelet Transforms with Controllable Redundancy." PhD thesis, Rice University, August 2001.

[61] S. Hatipoglu, S. K. Mitra, and N. G. Kingsbury. "Texture classification using dual tree complex wavelet transform." Image Processing And Its Applications, (465), pp. 344–347,1999.

[62] T. Heinonen, P. Dastidar, H. Frey, and H. Eskola. "Applications of MR Image Segmentation." International Journal of Bioelectromagnetism, 1(1), 1999.

[63] A. Jalobeanu, L. Blanc-Feraud, and J. Zerubia. “Satellite Image Deconvolution Using Complex Wavelet Packets.” Technical report, Institut National de Recherche en Informatique et en Automatique, France, 2000.

[64] H. Khalil and S. Shaheen. “Three Dimensional Video Compression.” IEEE Transactions on Image Processing, 8, pp. 762–773, June 1999.

[65] N. Kingsbury and J. Magarey. “Motion Estimation Using Complex Wavelets.” Technical report, Cambridge University Engineering Department, UK, 1995.

[66] N. G. Kingsbury. “The Dual–Tree Complex Wavelet Transform: A New Technique for Shift Invariance and Directional Filters.” Proceedings of the IEEE Digital Signal Processing Workshop, 1998.

[67] N. G. Kingsbury. “Image Processing with Complex Wavelets.” Phil. Trans. Royal Society London, 1999.

[68] N. G. Kingsbury and J. F. A. Magarey. “Wavelet Transforms in Image Processing.” First European Conference on Signal Analysis and Prediction, pp. 23–24, June 1997.

[69] Sheng-Tun Li, Shih-Wei Chou, and Jeng-Jong Pan. “Multi-resolution spatio-temporal data mining for the study of air pollutant regionalization.” 33rd Annual Hawaii International Conference on System Sciences(HICSS), 2000.

[70] P. Loo. “Digital Watermarking Using Complex Wavelets.” PhD thesis, Signal Processing and Communications Laboratory, University of Cambridge, 2002.

[71] L. Najman and M. Couprie. “Watershed algorithms and contrast preservation.” Discrete geometry for computer imagery, volume 2886 of Lecture Notes in Computer Science, pp. 62–71. Springer, 2003.

[72] J. Neumann and G. Steidl. “Dual–Tree Complex Wavelet Transform in the Frequency Domain and an Application to Signal Classification.”

International Journal of Wavelets, Multiresolution and Information Processing IJWMIP, 2004.

[73] P. Pinnamaneni and J. Meyer. “Three-dimensional Wavelet Compression.” 2nd Annual Tri-State Engineering Society Meeting, June 2001.

[74] O. Rioul and M. Vetterli. “Wavelets and signal processing.” IEEE Signal Processing Magazine, pp. 14–38, October 1991.

[75] I. W. Selesnick and K. Y. Li. “Video denoising using 2d and 3d dual–tree complex wavelet transforms.” Wavelets: Applications in Signal and Image Proc. X, 5207, pp. 607– 618, August 2003.

[76] J. Van De Vegte. “Fundamentals of Digital Signal Processing.” Prentice Hall, 2001.

[77] L. Vincent and P. Soille. “Watersheds in digital spaces: An efficient algorithm based on immersion simulations.” IEEE Transactions Pattern Analysis and Machine Intelligence, 13(6), pp. 583–593, 1991.

[78] Athanasios Nikolaidis and Ioannis Pitas. “Asymptotically Optimal Detection for Additive Watermarking in the DCT and DWT Domains.”, IEEE Transactions On Image Processing Vol.12,No.5, pp.563-571. 2003.

[79] Ahmed Bouridane ,Lahouari Ghouti ,Mohammad K. Ibrahim and Said Boussakta. “Digital Image Watermarking Using Balanced Multiwavelets.”, IEEE Transactions On Signal Processing Vol. 54, No. 4, pp. 1519-1536, April 2006.

[80] Chun-Hsien Chou and Kuo-Cheng Liu. “A Perceptually Tuned Watermarking Scheme for Color Images.”, IEEE Transactions On Image Processing Vol.19, No.11,pp. 2966- 2982, November 2010.

[81] Chih-Chin Lai and Cheng-Chih Tsai. “Digital Image Watermarking Using Discrete Wavelet Transform and Singular Value Decomposition.”, IEEE

Transactions On Instrumentation And Measurement Vol.59, No.11, pp. 3060-3063, November 2010.

[82] Chun-Shien Lu and Hong-Yuan Mark Liao. “Multipurpose Watermarking for Image Authentication and Protection.”, IEEE Transactions On Image Processing Vol. 10, No.10, pp.1579-1592, October 2001.

[83] Hua Yuan and Xiao-Ping Zhang. “Multiscale Fragile Watermarking Based on the Gaussian Mixture Model.”, IEEE Transactions On Image Processing Vol.15, No.10, pp.3189-3200, October 2006.

[84] Hu Zhihua, “Binary Image Watermarking Algorithm Based on SVD.”, International Conference on Intelligent Human-Machine Systems and Cybernetics pp.400-403, 2009.

[85] John, F. Doherty,YiweiWang, and Robert E. Van Dyck, “A Wavelet-Based Watermarking Algorithm for Ownership Verification of Digital Images.”, IEEE Transactions On Image Processing Vol.11, No.2, pp 77-88, February 2002.

[86] Liehua Xie and Gonzalo R. Arce, Fellow. “A Class of Authentication Digital Watermarks for Secure Multimedia Communication.”, IEEE Transactions On Image Processing Vol.10, No.11, pp.1754-1764, November 2001.

[87] Mauro Barni, Franco Bartolini and Alessandro Piva. “Improved Wavelet-Based Watermarking Through Pixel-Wise Masking” IEEE Transactions On Image Processing Vol.10, No.5, pp.783-791, May 2001.

[88] Ning Bi, Qiyu Sun, Daren Huang, Zhihua Yang, and Jiwu Huang. “Robust Image Watermarking Based on Multiband Wavelets and Empirical Mode Decomposition.”, IEEE Transactions On Image Processing Vol.16, No. 8, pp.1956-1966, August 2007.

[89] Ng, T. M. and Garg, H. K. “Maximum-Likelihood Detection in DWT Domain Image Watermarking Using Laplacian Modeling.”, IEEE Signal Processing Letters Vol.12, No.4, pp. 285-288, April 2005.

[90] Shih-Hao Wang and Yuan-Pei Lin. "Wavelet Tree Quantization for Copyright Protection Watermarking", IEEE Transactions On Image Processing Vol.16, No.8, pp.1956-1966, August 2007.

[91] Sabrina Lin, W. , Steven, K. Tjoa, H. Vicky Zhao and Ray Liu, K. J. Fello. "Digital Image Source Coder Forensics Via Intrinsic Fingerprints.", IEEE Transactions On Information Forensics And Security Vol.4,No.3,pp.460-475, September 2009.

[92] Xinge You, Liang Du, Yiu-ming Cheung and Qiuhui Chen. "A Blind Watermarking Scheme Using New Non tensor Product Wavelet Filter Banks.", IEEE Transactions On Image Processing, Vol.19, No.12, pp.3271-3284, December 2010.

[93] Zhe-Ming Lu, Dian-Guo Xu and Sheng-He Sun. "Multipurpose Image Watermarking Algorithm Based on Multistage Vector Quantization.", IEEE Transactions On Image Processing Vol.14,No.6, pp.822-831, June 2005.

[94] Chiou-Ting Hsu and Ja-Ling Wu. "Hidden Digital Watermarks in Images.", IEEE Transactions On Image Processing,Vol. 8, No. 1, pp 65-67, January 1999.

[95] Digital watermarking, http://en.wikipedia.org/wiki/watermarking.

[96] DWT materials, http://en.wikipedia.org/wiki/DWT

[97] Rafael C Gonzalez, Richard Eugene Woods. "Digital Image Processing (second edition).", Upper Saddle River, NJ,Prentice Hall, 2002

[98] Jillian Cannons, Pierre Moulin. "Design and Statistical Analysis of a Hash-Aided Image Watermarking System.", IEEE Transactions On Image Processing, Vol. 13, No. 10, October 2004.

[99] Masoud Alghoniemy and Ahmed H. Tewfik. "Geometric Invariance in Image Watermarking.", IEEE Transactions On Image Processing, Vol. 13, No. 2, February 2004.

[100] Nasir Memon and Ping Wah Wong. “A Buyer–Seller Watermarking Protocol.”, IEEE Transactions On Image Processing, Vol. 10, No. 4, April 2001.

[101] Gerrit C. Langelaar and Reginald L. Lagendijk. “Optimal Differential Energy Watermarking of DCT Encoded Images and Video.”, IEEE Transactions On Image Processing, Vol. 10, No. 1, January 2001.

[102] Liehua Xie and Gonzalo R. Arce. “A Class of Authentication Digital Watermarks for Secure Multimedia Communication.”, IEEE Transactions On Image Processing, Vol. 10, No. 11, November 2001.

[103] Changsheng Xu, Jiankang Wu, and Qibin Sun. “Audio registration and its application to digital watermarking. Security and Watermarking of Multimedia Contents.”, Proc.SPIE-3971, pp. 393–401, April 2000.

[104] G. Xuan, Y. Q. Shi, J. Gao, D. Zou, C. Yang, Z. Zhang, P. Chai, C. Chen, and W. Chen. “Steganalysis based on multiple features formed by statistical moments of wavelet characteristic functions.”, Proceedings 7th Information Hiding Workshop, Barcelona, Spain, June 6–8, 2005.

[105] G. Xuan, Q. Yao, C. Yang, J. Gao, P. Chai, Y. Q. Shi, and Z. Ni. “ Lossless data hiding using histogram shifting method based on integer wavelets.”, Proc. Int. Workshop on Digital Watermarking, volume 4283, pp. 323–332, November 2006.

[106] W. S. E. Yang and W. Sun. “On information embedding when watermarks and cover texts are correlated.”, IEEE International Symposium on Information Theory, pp. 346–350, 2006.

[107] Nakajima Yasumasa, Ichihara Shintaro, and Mogami Kazuto. “Digital camera and image authentication system using the same.”, Japanese Patent, JP 11215452, 1999.

[108] B.-L. Yeo and M. M. Yeung. “Watermarking 3D objects for verification.”, IEEE Computer Graphics and Applications, 19(1) pp. 36–45, 1999.

[109] M. Yeung and F. Mintzer. “An invisible watermarking technique for image verification.”, Proc. Int. Conf. Image Processing, volume 1, pp. 680–683, 1997.

[110] Gwo-Jong Yu, Chun-Shien Lu, H. Y. M. Liao, and Jang-Ping Sheu. “Mean quantization blind watermarking for image authentication.”, IEEE Int. Conf. on Image Processing, volume 3, pp. 706–709, 2000.

[111] M. El-Gayyar and J. von zur Gathen. “Watermarking techniques spatial domain.” University of Bonn Germany, Tech. Rep., 2006.

Author's Publications

[1] S P Ghrera and Rajesh Siddavatam, "A hybrid semi-blind digital image watermarking technique using lifting wavelet transform — Singular value decomposition" 2011 IEEE International Conference on Electro/Information Technology Minnesota State University Mankato USA, pp 1-6, 15 May - 17 May 2011. ieeexplore.ieee.org/iel5/5962075/5978551/05978552.pdf?...

[2] SP Ghrera, Rajesh Siddavatam, "An Intelligent Recursive Algorithm for 95% Impulse Noise Removal in Grey Scale and Binary Images using Lifting Scheme" in Journal:Lecture Notes in Engineering and Computer Science Year: 2011 Vol: 2193 Issue: 1, pp. 67-71 and Proceedings of World Congress on Engineering and Computer Science 2011(WCECS 2011), San Francisco, USA, 19 Oct – 21 Oct 2011.

www.doaj.org/doaj?func=abstract&id=864357&recNo=14&toc=1&uiLanguage=en
www.iaeng.org/publication/WCECS2011/WCECS2011_pp67-71.pdf

[3] SP Ghrera, Rajesh Siddavatam, " A Fast Progressive Image Transmission Algorithm Using Linear Bivariate Splines" SPRINGER International Journal of Communications in Computer and Information Science ISSN: 1865-0929, Contemporary Computing - Third International Conference, IC3 2010, Noida, India, Proceedings, Part I pp 568-578, August 9-11, 2010.
http://www.springerlink.com/content/lm4j507g330p325h/

[4] SP Ghrera, Rajesh Siddavatam, , "An Evolutionary Approach to Image Noise Cancellation Using Adaptive Particle Swarm Optimization (APSO) " Proceedings of IEEE International Conference on Computational Intelligence, Communication Systems and Networks (CICSyN 2010), Liverpool, UK, 28 Jul - 30 Jul 2010.
http://www.computer.org/portal/web/csdl/doi/10.1109/CICSyN.2010.20

Author’s Miscellaneous Publications

[1] S P Ghrera, Neetu Singh, Pranay Chaudhuri, “Denial of Service Attack:Analysis of Network Anomaly Using Queing Theory”, Published in the online proceedings of JOURNAL OF COMPUTER SCIENCE AND ENGINEERING Vol 1, Issue 1, May 2010.
http://sites.google.com/site/jcseuk/volume-1-issue-1-may-2010
http://arxiv.org/ftp/arxiv/papers/1006/1006.2807.pdf

[2] S P Ghrera, Amit Kumar Singh, “Level-2 Feature Extraction and Matching Algorithm Using Fingerprint Image”, Published in the proceedings of International Journal on Computer Engineering and Information Technology ISSN 0974-2034 IJCEIT, pp. 49-53, Vol 22, Issue 01, Dec 09-Feb 2010
http://www.serc.org.in/admin/pdffiles/6-VOL-22-IJCEIT.pdf

[3] S P Ghrera, Esha Kumar, Shivanka Chugh, “Performance Analysis of RED with different congestion control mechanisms”, Published in the proceedings of International Conference ETNCC 2011, 22-24 April 2011.
http://ieiudr.org/uploads/file/Etncc_Souvenir_Final%20Programme%5B1%5D.pdf

[4] S P Ghrera, “Green Computing”, Published in the online proceedings of 98th Indian Science Congress, SRM University, Chennai, January 3-7, 2011.
http://www.isc2011.in/pdf/engineering-sciences.pdf

[5] S P Ghrera, “ Security Architecture For SDR System Using OTA Download Sequence” published in the proceedings of The SDR08 Technical Conference, Washington DC, 26 Oct-30 Oct 2008.
http://groups.sdrforum.org/download.php?sid=1059

[6] S.P. Ghrera, Nitin Rakesh, Piyush Chauhan, Neetu Singh, “Team Spirit Model using standards for Video Delivery” Published in the proceedings of The National Conference on Recent Development in Computing and its Application (NCRDCA '09), Jamia Hamdard (Deemed University), New Delhi, pp.90-98,12 Aug- 13 Aug 2009.